January 2018

Synthesis And Characterization Of Novel Ni-Max And Alsi-Max Composites

Maharshi Dey

SYNTHESIS AND CHARACTERIZATION OF NOVEL NI-MAX AND ALSI-MAX COMPOSITES

by

Maharshi Dey

Bachelor of Technology (ME), West Bengal University of Technology, 2014

A Thesis

Submitted to the Graduate Facility

of the

University of North Dakota

In partial fulfillment of the requirements

For the degree of

Master of Science

Grand Forks, North Dakota

December

2018

This thesis, submitted by Maharshi Dey in partial fulfillment of the requirements for the Degree of Master of Science from the University of North Dakota, has been read by the Faculty Advisory Committee under whom the work has been done and is hereby approved.

_____

Dr. Surojit Gupta, Ph.D.

_____

Dr. Clement Tang, Ph.D.

_____

Dr. Yun Ji, Ph.D.

This thesis meets the standards for appearance, conforms to the style and format requirements of the School of Graduate Studies at the University of North Dakota, and is hereby approved.

_____

Grant McGimpsey

Dean of the School of Graduate Studies

_____

Date

PERMISSION

Title Synthesis and Characterization of Novel Ni-MAX and AlSi-MAX composites

Department Mechanical Engineering

Degree Master of Science

In presenting this thesis in fulfillment of the requirements for a graduate degree from the University of North Dakota, I agree that the library of this University shall make it freely available for inspection. I further agree that permission for extensive copying for scholarly purposes may be granted by the professor who supervised my thesis work or, in his absence, by the chairperson of the department or the dean of the School of Graduate Studies. It is understood that any copying or publication or other use of this thesis or part thereof for financial gain shall not be allowed without my written permission. It is also understood that due recognition shall be given to me and to the University of North Dakota in any scholarly use which may be made of any material in my thesis.

Name: Maharshi Dey

Date: 12.10.2018

TABLE OF CONTENTS

TABLE OF FIGURES

ACKNOWLEDGEMENTS

I am grateful to my colleagues, Matt Fuka and Faisal AlAnazi for their help and support. I am also grateful to Dr. Surojit Gupta at the University of North Dakota for the immense help and guidance I received during my studies. This work would not have been possible without anyone of them.

In addition, I would like to thank all the professors at the University of North Dakota who have taught me along the way and my friends and family who have helped me throughout my studies.

ABSTRACT

The main objectives of this thesis are: (a) synthesize and characterize Ni-Ti_3SiC_2 composites (Chapter 2), (b) understand and compare the effect of other MAX phases like Cr_2AlC, Ti_3AlC_2 and MoAlB on the mechanical and tribological behavior of Ni-matrix composites (Chapter 3), and (c) explore an alternative alloy to compare the tribological performance with Ni-Matrix composites (Chapter 4). This study shows that Ni-matrix composites can be fabricated by using a combination of cold pressing and subsequent hot pressing. All the composites were then studied by detailed microstructure investigations, mechanical, and tribological characterizations.

CHAPTER I

INTRODUCTION

1.1 SOLID LUBRICANTS AND NICKLE MATRIX COMPOSITES

Solid lubricants have become important engineering materials for reducing wear and friction coefficient between rotating components. Its potential usage can eliminate or reduce the reliance of oil-based machinery needed for oil lubrication. CaF_2, h-BN, WS_2, and graphite are some examples of solid lubricants which are currently being studied as additives in metal alloys for solid lubrication [1].

Ni is an important metal for designing different types of structural alloys. The demand for Ni has increased over the years. Amongst all, China has also become the largest consumer and importer of Nickel [2]. Similarly, Ni-matrix composites have also emerged as an important source for designing structural component due to their high mechanical strength couple with high wear resistance [3]. Hard particles like TiC can improve the wear resistance of pure Ni [3]. Ni-Matrix composites are also attractive as solid lubricants with additives like Ag, CaF_2/BaF_2 eutectic for high performance applications like foil bearings [4, 5]. A critical aim of this thesis is to explore novel solid lubricants, more particularly MAX phases as solid lubricants, in Ni-matrix composites (please see next section for details).

1.2 MAX PHASES

MAX Phases are layered, hexagonal, early transition-metal ternary carbides and nitrides [6]. Their chemical formula is $M_{n+1}AX_n$, where n = 1, 2, or 3, M is an early transition metal, A is a group A element, and X is carbon or nitrogen (Fig. 1.1) [6-8]. These phases have characteristics reminiscent of both metals and ceramics, for example, they are excellent thermal and electrical temperatures. However, like a ceramic, it is oxidation resistant, extremely refractory, and able to

maintain strength at elevated temperatures [6]. Different groups have reported promising behavior of properties of MAX-metal composites [8-11]. Kothalkar et al. [8] reported an enhancement by 1.5 times in yield strength in AA6061/Ti_2AlC composites as compared to peak aged AA6061. Kothalkar et al. [9] also studied equiatomic NiTi and Ti_3SiC_2 and observed extraordinarily high damping in both thermo-mechanically cycled and as-sintered composites until 200 MPa. Agne et al. [10] presented a fundamental study that Al-V_2AlC composites can be fabricating by quenching rather than furnace cooling. The research group at University of North Dakota led by Prof. Gupta has explored the use of these phases as particulates in metal and polymer matrices [12-19].conductivity, easily machinable, relatively soft, resistant to thermal shock, and plastic behavior at higher

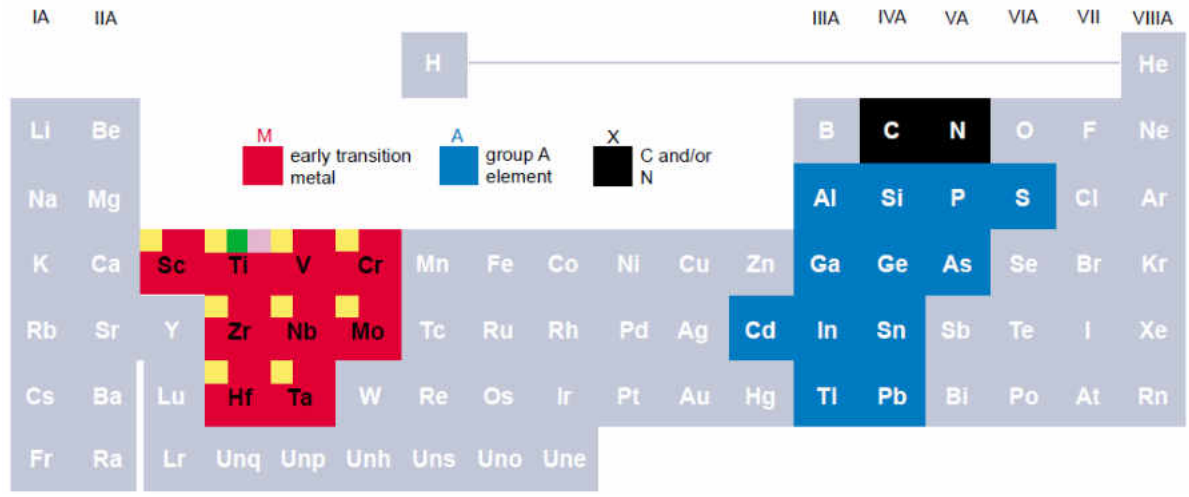

Figure 2.1: MAX phases are made up of M – early transition metal (red), A – element from the A groups (blue), and X – carbon or nitrogen (black). Their chemical formula is $M_{n+1}AX_n$, where n = 1, 2, or 3, and each respective group is known as 211, 312, or 413 [7]

1.3 MAX REINFORCED METALS (MRMS)

Metal matrix composites that are reinforced with MAX phase will be referred to MAX reinforced metals (MRMs) in this thesis. In previous studies, the addition of MAX phases has shown improvement in the mechanical and tribological properties of different metal matrices like Al, Sn, Zn, Ag, and Bi [12-15]. The beneficial effects of adding Ti_3SiC_2 to various metal matrices is summarized in the Figs. 1.2 and 1.3 [15]. MAX phase particulates have also shown beneficial effects on the mechanical and tribological performances in polymer matrices [19-21]. These composites are called MAX reinforced polymers (MRPs). These can be used in potential applications where excellent tribological performances of polymer matrix composites are desired. The main objectives of this thesis are: (a) synthesize and characterize Ni-Ti_3SiC_2 composites (Chapter 2), (b) understand and compare the effect of other MAX phases like Cr_2AlC, Ti_3AlC_2 and MoAlB on the mechanical and tribological behavior of Ni-matrix composites (Chapter 3), and (c) explore an alternative alloy to compare the tribological performance with Ni-Matrix composites (Chapter 4).

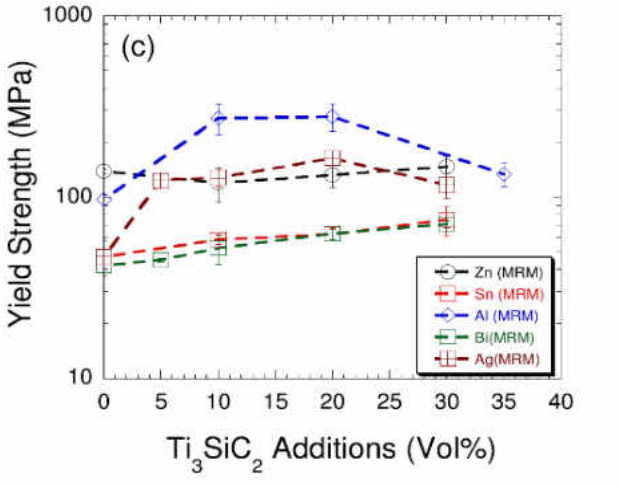

Figure 1.2: Plot of stress versus displacement of yield strength of different MRMs versus Ti_3SiC_2 content [15].

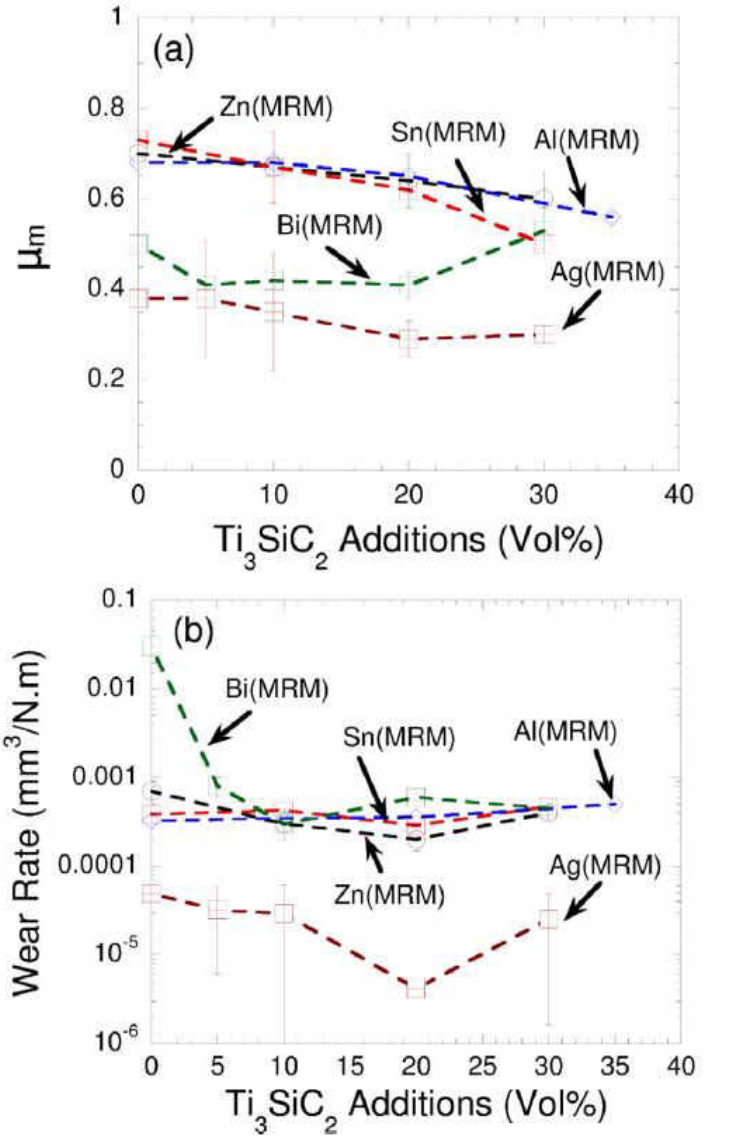

Figure 1.3: Plot of MRMs (a) μ_m, and (b) wear rates as a function of Ti_3SiC_2 content [15].

CHAPTER II

SYNTHESIS AND CHARACTERIZATION OF NOVEL NI-TI_3SIC_2 COMPOSITES

This work has been published in the Proceeding of the 42nd International Conference on Advanced Ceramics and Composites, Ceramic Engineering and Science Proceedings Volume 39, Issue 2, 2018, "Synthesis and Characterization of Novel Ni-Ti_3SiC_2 Composites", M. Dey, M. Fuka, F. AlAnazi, and S. Gupta.

2.1 INTRODUCTION

Nickel is an important material for various engineering applications due to its unique properties like magnetism, strength, corrosion resistance, and wear resistance [1]. The wear resistance of Ni can be further improved by adding dispersed hard particles like SiC, TaC, and NbC into the Ni matrix [1-3]. These composite materials and coatings are promising materials for protection of tribological components, low cost coatings for replacement of hard Chromium coatings, among other applications [1-3]. Ni-matrix composites have also attracted a lot of attention for their potential usage as solid lubricants by incorporating various additives like Ag, and CaF_2/BaF_2 eutectic for high performance applications like foil bearings [4-6]. Based on these results, it can be hypothesized that lubricious particulates like MAX Phases can be promising additive for enhancing the functional attributes of the Ni and Ni-based alloys.

As a background, it is now well established that $M_{n+1}AX_n$ (MAX) phases, where n =1,2,3; M is an Early Transitional Metal, A is a Group A element (mostly groups 13 and 14); and X is C and/or N, are novel ternary carbides and nitrides which have excellent properties like damage

tolerance, thermal shock resistance and machinability [7-11]. Gupta et al. [12-15] have showed that the addition of MAX phase (Ti_3SiC_2) particulates have enhanced the mechanical and tribological performance of Al-, Sn-, Zn-, Bi- and Ag-matrix composites. The authors have classified these new generation of composites as MRM (Metal Reinforced with MAX) as 5-30 vol% Ti_3SiC_2 was used to reinforce the metal matrix. A major hurdle for designing Ni-Ti_3SiC_2 composites is the propensity of reaction between Ni and Ti_3SiC_2 phases at 1450 ^oC during the sintering process [16]. The goal of this paper is to report the synthesis and characterization of novel Ni-Ti_3SiC_2 composites at lower temperatures by hot pressing.

2.2 EXPERIMENTAL

Ti_3SiC_2 powder (-325 mesh, Kanthal, Hallstahammar, Sweden) and calculated concentrations of Ni powders (Part number 43214 (-325 mesh and 99.8% pure), Alfa Aesar, Haverhill, MA) were dry ball milled (8000 M mixer Mill, SPEX SamplePrep, Metuchen, NJ) for 2 minutes. All the mixed powders were then poured in a die and then hot pressed (HP) under a uniaxial compressive stress of ~240 MPa (~12.7 mm die) at 600 ^oC for 5 minutes. For comparison, samples of pure Ni were also fabricated by following the above-mentioned procedure at ~240 MPa (Ni (240 MPa)) and ~165 MPa (Ni (165 MPa)), respectively. Ni-based MRM composites were designed by adding 5 vol% (Ni-5%312Si), 10 vol% (Ni-10%312Si), 20 vol% (Ni-20%312Si) Ti_3SiC_2, and 30 vol% (Ni-30%312Si) Ti_3SiC_2 in the Ni- matrix. Theoretical density of Ti_3SiC_2 and Ni particulates were used to calculate the theoretical density (ρ_T) of all the composite samples by using the rule of mixture calculations. The experimental density (ρ_E) of the composites was then calculated from the mass and dimensions of each sample. Thereafter, the porosity (P) of the sample was determined by the Eq, 1.

$$P = \left(1 - \frac{\rho_E}{\rho_T}\right) \text{ x } 100 \text{ ----------(I)}$$

For each composition, a set of 5 samples were then tested in compression by using a mechanical testing unit (Shimadzu AD-IS UTM, Shimadzu Scientific Instruments Inc., Columbia, MD) at a deflection rate of 1 mm/min on cube samples (~3 mm x ~3 mm x ~3 mm) which were machined by a diamond saw from the hot-pressed samples.

Due to experimental limitations, stress versus displacement plots are reported as the actual strain during mechanical testing could not be determined. In the paper, the yield strength is defined when stress versus displacement plot transitions from the linear to non-linear regime. The linear region of the composites had a regression fitting of $R^2 > 0.95$. For each composite, an average of 5 yield strength measurements is reported in the text [12-15]. Vicker's micro-hardness indentor (Mitutoyo HM-112, Mitutoyo Corporation, Aurora, IL) was performed by loading the samples at 4.9 N for 12 s. In the text, an average of at least five readings for each composite system is reported. XRD measurements were performed on the samples by using a Rigaku Diffractometer (SmartLab, Rigaku, Japan) at a scan rate of 4 °/min from 20° to 50°. The tribological behavior of the samples were investigated by using a ball-on-disc tribometer (CSM Instruments SA, Peseux, Switzerland) against alumina (Al_2O_3 balls (~6 mm diameter), Anton Paar USA Inc., Ashland, VA) and stainless steel (SS) (100Cr6 (~6 mm diameter), Anton Paar USA Inc., Ashland, VA). The experiment conditions used during these studies were 5 N, ~31.4 cm/s linear speed, ~5 mm track radius, and a sliding distance of 200 m and 1000 m for testing the composites against SS and Al_2O_3 balls, respectively. All the Ni-Ti_3SiC_2 disks were also polished to a ~1 µm finishing which were confirmed by using a surface profilometer (Surfcom 480A, Tokyo Seimitsu Co. Ltd., Japan). After performing the tribological testing for each composition, the μ_{mean} was then calculated by averaging the mean results obtained from the three and five data sets of similar Ni-Ti_3SiC_2 composition during sliding against SS and Al_2O_3, respectively. The mass of the samples and

substrates were measured before and after the testing by using a weighing scale (Model XA82/220/2X, Radwag Balances and Scales, Poland). The specific wear rate (WR) was calculated from:

$$WR = (m_i - m_f)/(\rho.N.d) \quad \text{----------(II)}$$

where, m_i is the initial mass, m_f is the final mass, ρ is density of the composite, N is the applied load, and d is the total distance traversed by the sample during the tribology testing. The total WR from both the counterparts is reported in the text. The methodology for inspecting the tribosurfaces are reported in Chapters 2 and 3.

2.3. RESULTS AND DISCUSSION

2.3.1 MICROSTRUCTURE AND PHASE ANALYSIS

SEM images of Ni-Ti_3SiC_2 composites are shown in Fig. 1. In all the compositions, Ti_3SiC_2 particulates are well-dispersed in the Ni matrix. The inspection of the interface between Ni and Ti_3SiC_2 particles even at higher magnifications did not show any discernible interfacial reaction (Fig. 1f). XRD plots of Ni-Ti_3SiC_2 composites also show predominantly Ni and Ti_3SiC_2 peaks (Fig. 2). By analyzing the Figs. 1 and 2, it can be construed that Ti_3SiC_2 particulates have minimal reaction with the Ni-matrix. Further TEM studies are recommended to study the interfaces of Ni and Ti_3SiC_2 particulates (currently, this facility is beyond the experimental capability of the authors). Figure 3 plots the variation of porosity as a function of Ti_3SiC_2 content. When the Ti_3SiC_2 content was varied between 5 and 20 vol%, the Ni-Ti_3SiC_2 composites had similar porosity of ~12%, for example, Ni-5%312Si had a porosity of ~11.8% and Ni-20%312Si had porosity of ~12.5%. Comparatively, Ni and Ni-30%312Si fabricated under similar conditions had porosity of ~9.82% and ~17.7%, respectively. For comparison, Ni (165 MPa) had a porosity of ~17.7% (Fig.

3a). In general, samples fabricated by hot pressing showed higher density than the samples fabricated by pressureless sintering [12-15]. The hardness of Ni-Ti_3SiC_2 composites retained similar values of ~1.58 GPa in Ni to ~1.53 GPa in Ni-5%312Si although the former sample was denser, thereafter it decreased from ~1.47 GPa in Ni-10%312Si to 1.26 GPa in Ni-30%312Si (Fig. 3b). Among all the MRMs studied so far, Ni-based MRMs showed the highest hardness (Fig. 3c).

2.3.2 COMPARISON OF MECHANICAL PERFORMANCE OF MRMS

Figures 4 shows the plot the compressive strength versus displacement plots of different Ni-Ti_3SiC_2 composites. At lower concentration until ~10 vol% of the Ti_3SiC_2 additions, the addition of Ti_3SiC_2 particulates in the matrix compressive did not have any appreciable effect on the mechanical performance, but after addition of higher concentration of Ti_3SiC_2, the failure become more brittle in nature. Figure 4b summarizes the yield strength of Ni-Ti_3SiC_2 composites for better understanding of the mechanical behavior of these composites. More particularly, the mean yield strength of Ni-Ti_3SiC_2 composites varied from ~600 MPa in Ni to ~592 MPa in Ni-5%312Si, thereafter, it decreased gradually to ~465 MPa in Ni-20%312Si, and then it sharply decreased to ~227 MPa in Ni-30%312Si. Comparatively, the yield strength of Ni (165 MPa) was ~467 MPa. Clearly, porosity and Ti_3SiC_2 are both contributing to the mechanical performance, and more studies are needed to delineate the effect of these two factors. Comparably, the yield strength of the other MRMs was significantly lower (Fig. 4c). These results show that by tailoring the particulate content and the metal matrix, it is quite possible to engineer the mechanical behavior of these composites according to the strength requirement for a specific design.

2.3.3 SUMMARY OF TRIBOLOGICAL BEHAVIOR OF DIFFERENT MRMS

Figures 5a and 5b show the plot of friction coefficient (μ) versus distance of Ni-Ti_3SiC_2 composites sliding against alumina and SS balls, respectively. While sliding against Al_2O_3, Ni-Ti_3SiC_2 composites attained steady state after cycling for ~200 m although Ni-30%312Si showed some fluctuations (Fig. 5a). Comparatively, Ni-Ti_3SiC_2 composites sliding against SS balls showed greater fluctuations, but by qualitatively inspecting the plots, it can be surmised that the addition of Ti_3SiC_2 has increased the μ (Fig. 5b). For detailed analysis, Figs. 6a and b plot the WR and μ as a function of Ti_3SiC_2 content. During sliding against SS, the addition of Ti_3SiC_2 particulates marginally decreased the WR from ~0.003 mm^3/N.m in Ni to ~0.002 mm^3/N.m in Ni-10%312Si, thereafter the composites retained similar WR values until Ni-30%312Si (Fig. 6a). The μ_{mean} was ~0.55 in Ni, thereafter, it retained similar value of ~0.54 in Ni-5%312Si, and then it increased to ~0.78 in Ni-10%312Si. Thereafter, the μ_{mean} increased to ~0.86 in Ni-30%312Si (Fig. 6b). In other words, this study shows that the addition of ~5 vol% Ti_3SiC_2 can marginally reduce the adhesive wear in Ni-Ti_3SiC_2/steel tribocouple without affecting the μ. More studies are needed to optimize the particle size and concentration of Ti_3SiC_2 particulates as higher amount of Ti_3SiC_2 additions (>10 vol%) increased the μ without having drastic effect on the WR.

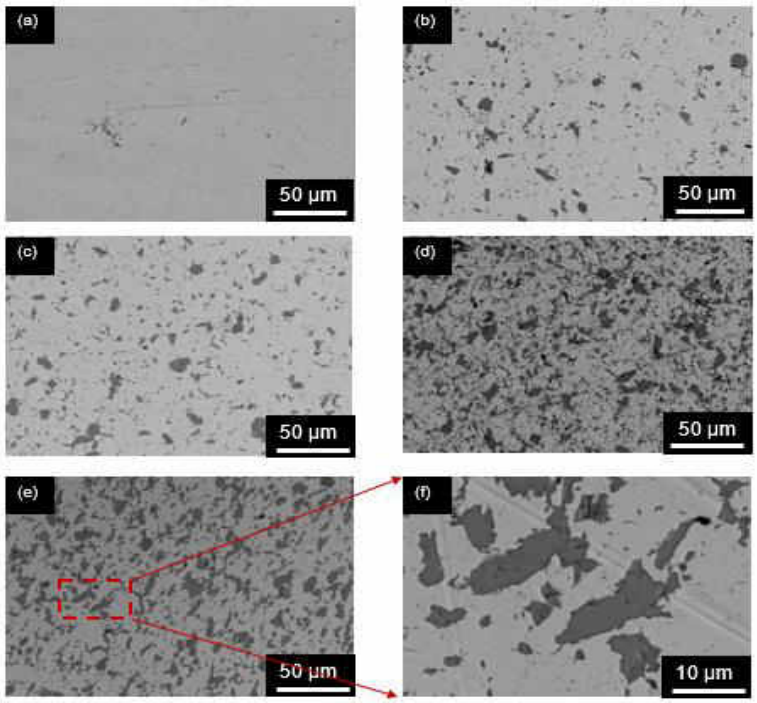

Figure 2.1: SEM SE micrograph of, (a) Ni, and BSE images of, (b) Ni-5%312Si, (c) Ni-10%312Si, (d) Ni-20%312Si, (e) Ni-30%312Si, and (f) higher magnification of the region marked in (e).

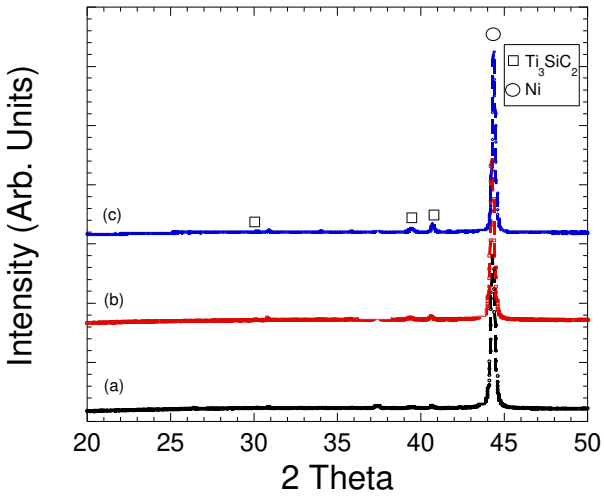

Figure 2.2: XRD profiles of, (a) Ni-5%312Si, (b) Ni-10%312Si, and (c) Ni-20%312Si

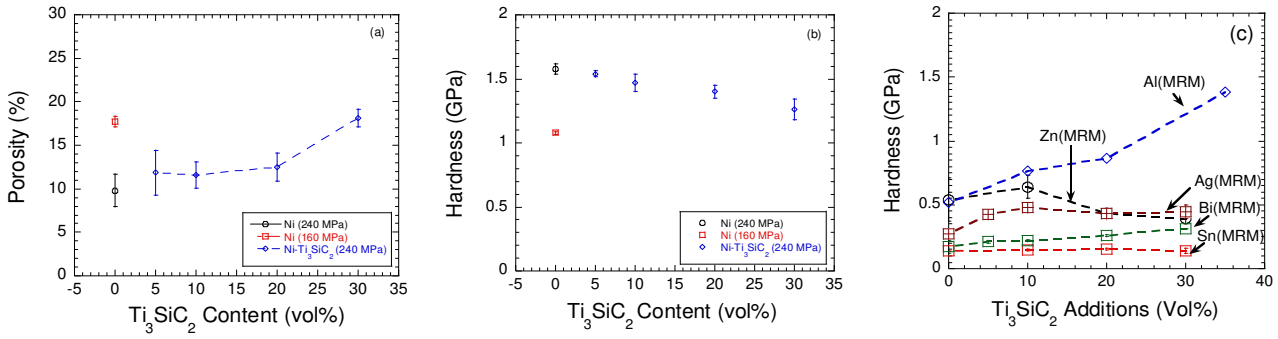

Figure 2.3: Plot of, (a) porosity, and (b) hardness versus Ti_3SiC_2 content, and hardness versus Ti_3SiC_2 content of different MRMs studied in a previous work [15].

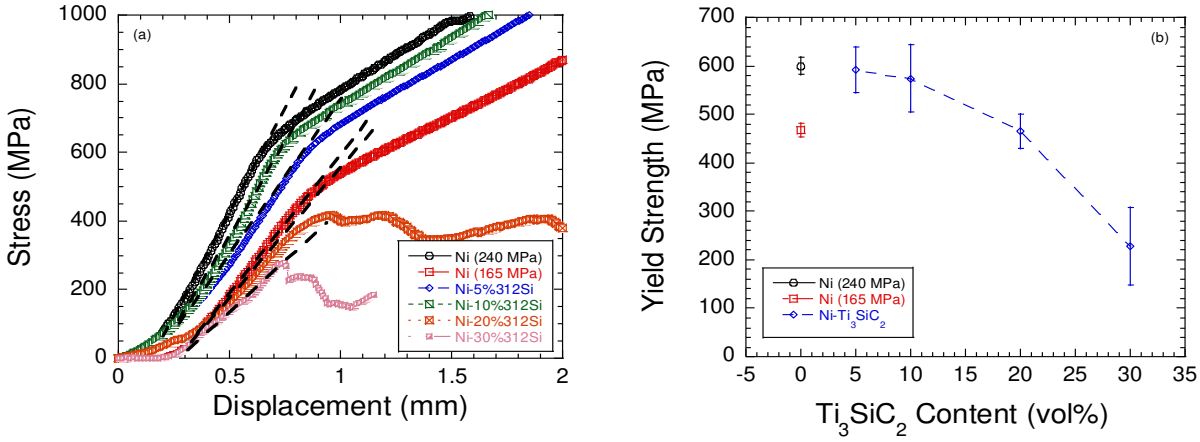

Figure 2.4: Plot of, (a) stress versus displacement profile of Ni-Ti_3SiC_2 composites, and (b) yield strength versus Ti_3SiC_2 content.

Comparatively, during sliding against Al_2O_3, Ni had a WR of ~2.95 x 10^{-5} mm^3/N.m, and the WR marginally decreased to ~2.42 x 10^{-5} mm^3/N.m in Ni-5%312Si, thereafter the WR increased gradually to ~3.96 x 10^{-5} mm^3/N.m in Ni-10%312Si, and then increased sharply to ~1.78 x 10^{-3} mm^3/N.m and 8 x 10^{-4} mm^3/N.m in Ni-20%312Si and Ni-30%312Si, respectively (Fig. 6a). The μ_{mean} was ~0.36 in Ni, thereafter, it gradually increased to ~0.54 in Ni-10%312Si, and retained similar values until Ni-30%312Si (Fig. 6b). This study shows that the addition of ~5 vol% Ti_3SiC_2 can marginally reduce the abrasive wear without drastically affecting the μ. The addition of 10 vol% and higher concentration of Ti_3SiC_2 increased both the WR and μ. It was shown in the last section that the additions of Ti_3SiC_2 makes the composites brittle as compared to the pristine Ni matrix (Fig. 4b). The higher WR at >10 vol% Ti_3SiC_2 addition can be explained by the inherent brittleness of the composite which renders it more vulnerable to the abrasive wear.

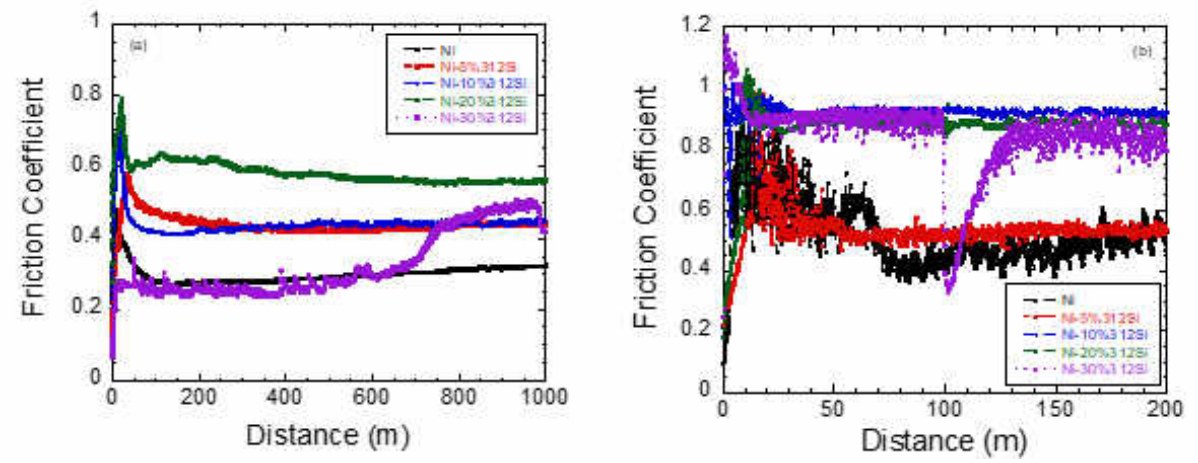

Figure 2.5: Plot of friction coefficient (μ) versus distance of Ni-Ti_3SiC_2 tribocouples against, (a) alumina, and (b) SS.

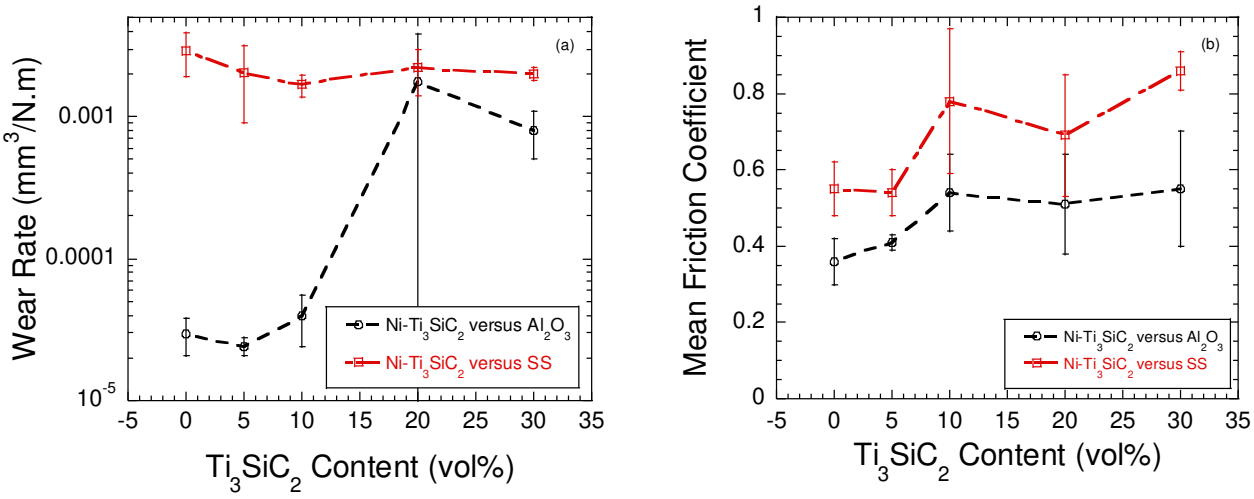

Figure 2.6: Plot of, (a) WR, and (b) mean friction coefficient (μ_m) versus Ti_3SiC_2 content.

2.3.4 STUDY OF TRIBOFILMS AND MECHANISM OF WEAR

Figure 7 shows the SE SEM micrographs of the Ni-10%312Si (Figs. 7a-b) and alumina surface (Figs. 7c-d) after tribology testing. Both the surfaces are covered with tribofilms which are created due to the wear and subsequent oxidation of Ni-10%312Si surface, for example, the presence of sub-stoichiometric micro constituents $*Ni_{0.87}Al_{0.06}Ti_{0.05}Si_{0.02}O_{0.61}\{C_x\}*$ (Fig. 7b) and $*Ni_{0.92}Al_{0.03}Ti_{0.03}Si_{0.01}O_{0.25}\{C_x\}^*$ (Fig. 7d) on Ni-10%312Si and alumina surface, respectively. By analyzing the tribochemistry of SEM images, it can be construed that the Ni-based MRMs are mainly contributing to the formation of tribofilms. Figure 8 shows the tribosurfaces of SS (Figs. 8 a-b) and Ni-5%312Si (Figs. 8 c-d). Both the surfaces showed Ni-rich sub-stoichometric oxides which shows that mainly Ni-Ti_3SiC_2 composite surface is contributing to the formation of tribofilms. According to the classification developed by Gupta and Barsoum [17] tribofilms can be classified as Type IV tribofilms where MAX based composites contribute to the formation of tribofilms. Based on the architecture of the tribofilms, Gupta and Barsoum [17] further divided the Type IV tribofilms into several sub-categories, namely: (a) Type IVa tribofilms (lubricous and

chemically homogenous at the microscale) [17], (b) Type IVb tribofilms (decomposed Ag-rich regions mixed with different triboxides) (Fig. 12b) [17], and (c) Type IVc tribofilms (powdery) [12]. The tribofilms formed in Ni-Ti_3SiC_2 and alumina or stainless steel tribocouples are lubricious (when the Ti_3SiC_2 content is ≤10 vol%), thus by using the classification above, the tribofilms can be classified as Type IVa.

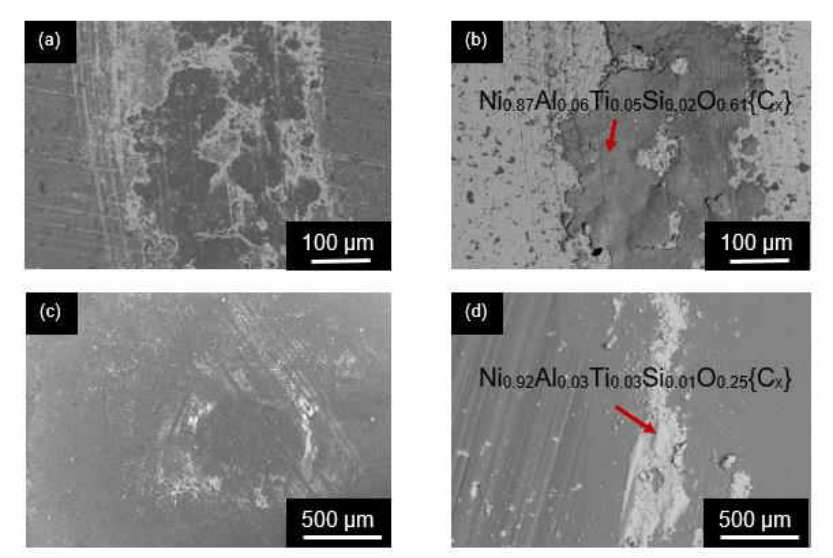

Figure 2.7: SEM micrographs of, (a) Ni-10%312Si (SE), (b) BSE image of the same region, (c) alumina surface, and (d) alumina surface at higher magnification (BSE).

In summary, the addition of 5-10 vol% of Ti_3SiC_2 particulates has some beneficial effect on the tribological behavior without having an adverse effect on the mechanical behavior thereafter both the tribological and mechanical properties detoriate at higher concentration of Ti_3SiC_2 particulates. Table 1 summarizes the tribological behavior of different Ni-based solid lubricants. The WR of well-studied solid lubricant compositions like PS300, PS400, and NAF 5 lies in the range of 10^{-3}-10^{-5} mm^3/N.m. These solid lubricants are also composed of multiple constituents (Table 1). Clearly, Ni-Ti_3SiC_2 composites offer a new alternative for Ni-based solid lubricants

with the inherent advantage that the composition is simpler, and can be potentially deposited into coatings. More studies are needed to understand the high temperature lubrication behavior of these composites.

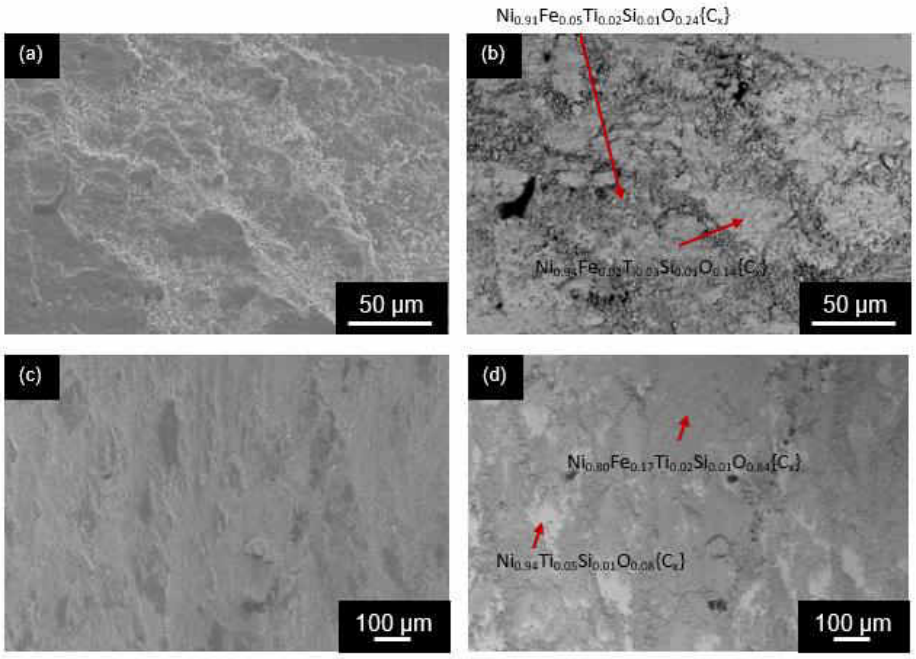

Figure 2.8: SEM micrograph of, (a) SS surface (SE), (b) BSE image of the same region, (c) Ni-5%312Si surface (SE), and (d) BSE image of the same region.

Table 1.1: Summary of tribological behavior of different Ni-based coatings and composites

Coatings /Compositions	**Countersurface**	**Conditions**	**WR**	**μ**	**Ref.**
PS300 (NiCr-Cr_2O_3 (80.3 vol%), Ag (5.5 vol%), CaF_2/BaF_2 (14.2 vol%))	Al_2O_3 (pin)	Pin-on-disk, RT, 4.91 N, and 1 m/s	~2.3 x 10^{-4} (total wear)	0.62	4
PS400 (NiMoAl (70 wt%)-Cr_2O_3 (20 wt%)-Ag (5 wt%) - BaF_2/CaF_2(5 wt%))	Inconel X-750 (pin)	Pin-on-disk, RT, 4.91 N, and 3 m/s after previous sliding at 500 °C and 650 °C	~1.1 x 10^{-3} (total wear)	0.31	5
NAF5 (Ni-alloys–12.5%Ag–5%BaF_2/CaF_2)	Si_3N_4 ball	Ball-on-Disk, RT, 5 N, and 1 m/s	~6 x 10^{-5} (WR of NAF5)	0.3	6
NAF10 (Ni-alloy-12.5%Ag-10%BaF_2/CaF_2)			~7 x 10^{-5} (WR of NAF10)	0.32	
NAF15 (Ni-alloy-12.5%Ag-15%BaF_2/CaF_2)			~10^{-4} (WR of NAF15)	0.35	
NAF5 (Ni-alloys–12.5%Ag–5%BaF_2/CaF_2)	Inconel 718		~5 x 10^{-5} (WR of NAF5)	0.32	
NAF10 (Ni-alloy-12.5%Ag-10%BaF_2/CaF_2)			10^{-4} (WR of NAF10)	0.34	
NAF15 (Ni-alloy-12.5%Ag-15%BaF_2/CaF_2)			~8 x 10^{-5} (WR of NAF10)	0.35	

2.4. CONCLUSIONS

Ni-Ti_3SiC_2 composites were fabricated by hot pressing. The microstructure evaluation showed that Ti_3SiC_2 particulates are well dispersed in the microstructure with minimal interfacial reactions. The mean yield strength of Ni-Ti_3SiC_2 composites varied from ~600 MPa in Ni to ~592 MPa in Ni-5%312Si, thereafter, it decreased gradually to ~465 MPa in Ni-20%312Si, and then it sharply decreased to ~227 MPa in Ni-30%312Si. Ti_3SiC_2 particulates had a beneficial effect on the tribological behavior. More particularly, it was observed that the addition of 5-10 vol% Ti_3SiC_2 can help in mildly reducing both the adhesive and abrasive wear, but at higher concentrations, the composites were found to be more vulnerable towards abrasive wear as compared to adhesive wear due to brittle nature of the composites. The tribofilms formed during the dry sliding of Ni-Ti_3SiC_2 composites against both SS and alumina were further investigated by SEM and X-ray analysis and were further classified into Type IVa tribofilms.

2. 5. Acknowledgements

One of the authors (SG) would like to acknowledge the CRADA between UND and ARL for support. Authors would also like to thank Kanthal Inc. for supplying the Ti3SiC2 powders. NDSU Electron Microscopy Center core facility is also acknowledged for the microscopy. This material is also based upon work supported by the National Science Foundation under Grant No. 0619098, and 1229417. Any opinions, findings, and conclusions or recommendations expressed in this material are those of the author(s) and do not necessarily reflect the views of the National Science Foundation.

CHAPTER III

SYNTHESIS AND CHARACTERIZATION OF NOVEL NI-MAX COMPOSITES

3.1 EXPERIMENTAL

Ti_3AlC_2 powders were fabricated by mixing powders of TiH_2 (Part number 209279 (-325 mesh and 98% pure), Sigma-Aldrich, St. Louis, MO), Al (Part number 11067 (7-15 micron powder and 99.5% pure), Alfa Aesar, Haverhill, MA) and TiC (Part number 40178 (~2 micron powder and 99.5% pure), Alfa Aesar, Haverhill, MA) in 1:1.1:2 molar ratio. The powers were then dry mixed for 5 minutes in a ball mill (8000 M mixer Mill, SPEX SamplePrep, Metuchen, NJ) in a methacrylate vial with methacrylate balls. The powders were further mixed with 10 wt% PVA for 10s. The mixed powders were then poured in a ~25.4 mm die and then cold pressed (Model 3853-0, Carver, INC., Wabash, IN) at ~88 MPa to make compact pellets. The pellets were then annealed at 750 ^oC for 2h and then heated up to 1400^oC for 2h at a heating rate of 10 ^oC/min. Similarly, Cr_2AlC powders were fabricated by mixing Cr (Part number 266299 (-325 mesh and ≥99% trace metal basis), Sigma-Aldrich, St. Louis, MO), Aluminum (Lot KO5Z034 (-325 mesh, 99.5% trace metal basis), Alfa Aesar, Haverhill MA), and Carbon (LotY19B065 (Graphite powder crystalline, (-325 mesh and 99% pure)), Alfa Aesar, Haverhill MA) in a molar ratio of 2:1.1:1. The powders were then ball milled for 5 mins in a methacrylate vial with methacrylate balls. The mixed powders were then poured in a ~25.4 mm die and cold pressed (Cold press, model 3853-0, Carver, INC., Wabash, IN) at ~88 MPa to make compact pellets. This pellet was then heated at 1350 ^oC for 4 h.

The sintered pellets of both compositions were then ball milled (8000 M mixer Mill, SPEX SamplePrep, Metuchen, NJ) for 30 min in an 8001B hardened steel vial with 8001B hardened steel balls. The resultant powders were then sieved until -325 mesh in a sieve shaker. XRD measurements, performed by a Rigaku Diffractometer (SmartLab, Rigaku, Japan) at a scan rate of 4 ^{o}/min from 20^{o} to 50^{o} confirmed single phase Ti_3AlC_2 and Cr_2AlC powders.

In this study, 5 vol%, 10 vol%, 20 vol%, and 30 vol% of Ti_3AlC_2 and Cr_2AlC particulates were used as a reinforcement in the Ni-matrix composites. They will be referred to by using the following nomenclature, Ni-xvol%Ti_3AlC_2 or Ni-xvol%Cr_2AlC. For example, Ni-20vol%Cr_2AlC means that Ni matrix is reinforced with 20 vol% Cr_2AlC. For fabricating composites, calculated amounts of Ti_3AlC_2 (-325 mesh) or Cr_2AlC (-325 mesh), and Ni powders (Part number 43214 (-325 mesh and 99.8% pure) Alfa Aesar, Haverhill, MA) were mixed in a ball mill (8000 M mixer Mill, SPEX SamplePrep, Metuchen, NJ) for 5 minutes. The mixed powders were then cold-pressed at ~263 MPa in metal die (~12.7 mm diameter) then the samples were hot-pressed under a uniaxial compressive stress of ~240 MPa at 600 ^{o}C for 5 minutes. For comparison, Ni sample was also manufactured by the same route. This composition will be referred to as Ni (A-composition). In an earlier study, Ni samples were also synthesized under similar hot press conditions, but the compacts were cold pressed at ~88 MPa. This composition will be referred to as Ni (B-composition) [1]. The mass and dimensions of all the samples were measured to determine the experimental density (ρ_E). The theoretical density of the Ti_3AlC_2, Cr_2AlC and Ni particulates were used to calculate the theoretical density (ρ_T) of the composites by rule of mixtures. Thereby, the relative density of the composites were calculated by dividing the experimental density with the theoretical density of the samples. Porosity (P) of the sample was then determined by the Eq, 1.

$$P = \left(1 - \frac{\rho_E}{\rho_T}\right) \text{x } 100 \text{ ----------(I)}$$

The characterization techniques for mechanical testing by uniaxial compression, XRD for phase analysis, and hardness are mentioned in the Chapter II except tribology measurements. The tribology characterization was done by using SS balls as a tribo-partner in this by ball on disc method. All the other parameters are similar to Chapter II.

3.2 RESULTS AND DISCUSSION

3.2.1 MICROSTRUCTURE AND PHASE ANALYSIS

BSE SEM images of the MAX Phase powders Ti_3SiC_2, Ti_3AlC_2 and Cr_2AlC are shown in Figs. 1 a-c, respectively. The SEM micrographs of Ni-Cr_2AlC and Ni-Ti_3AlC_2 composites are shown in Fig. 2 and Fig. 3, respectively. All the compositions showed that MAX phase particulates are evenly distributed the Ni matrix. Moreover, no interfacial reactions were observed even at higher magnifications between Ni and Cr_2AlC (Fig. 3.2f) or Ti_3AlC_2 (Fig. 3.3f). XRD plots of these two composites are summarized in Fig. 4. All the compositions showed peaks of Ni and MAX particulates which further corroborates the SEM findings.

Figure 5 plots porosity versus the content of the MAX or MoAlB phase reinforcement in the Ni-Matrix. The Ni (A-composition) fabricated during study has ~9.82% porosity as compared to ~13% porosity in Ni (B-composition) [1]. This study shows that high cold pressing pressure is a critical requirement for manufacturing dense compositions by using the procedure mentioned above. Thus, the Ni-Ti_3AlC_2 and Ni-Cr_2AlC compositions fabricated during study are denser than Ni-MoAlB compositions fabricated during a previous study [1]. For example, Ni-5%Cr_2AlC, Ni-10%Cr_2AlC, and Ni-20%Cr_2AlC had similar porosities of ~10.7%, ~10.8%, and ~10.9%, respectively. The composition Ni-30%Cr_2AlC had a higher porosity of ~19.6% porosity. Similarly, Ni-5%Ti_3AlC_2, Ni-10%Ti_3AlC_2, and Ni-20% Ti_3AlC_2 had porosities of 9.8%, 11.8%, and 12.7%, respectively. Like the former case, the composition Ni-30%Ti_3AlC_2 had a higher porosity of

~19.6% porosity. Comparatively, Ni-5%Ti_3SiC_2, Ni-10%Ti_3SiC_2, Ni-20% Ti_3SiC_2 and Ni-30% Ti_3SiC_2 composites fabricated by similar method had porosities of ~11.8%, ~11.6%, ~12.5% and ~18.1%, respectively (Chapter 2). This study shows that the densification of Ni-MAX composites are showing a similar trend during manufacturing by using a combination of cold pressing and hot pressing.

Figure 5b shows the plot of hardness versus MAX or MoAlB content. Both the Ni compositions had similar hardness of ~1.6 GPa. For Ni-Ti_3AlC_2 compositions, the hardness decreased slightly from ~1.5 GPa in Ni-5%Ti_3AlC_2 to ~1.4 GPa in Ni-20%Ti_3AlC_2, respectively. The hardness of Ni-30%Ti_3AlC_2 composite decreased to ~1.1 GPa. For Ni-Cr_2AlC composites, the hardness retained a value of ~1.5 GPa until Ni-10%Cr_2AlC composite, thereafter it decreased to ~1.4 GPa in Ni-20%Cr_2AlC and ~1.1GPa in Ni-30%Cr_2AlC composites. For comparison, Ni-Ti_3SiC_2 composites also showed a similar trend (Fig. 5b).

3.2.2 COMPARISON OF MECHANICAL PERFORMANCE OF MRMS

Figures 3.6a and 3.6b show the plots for the compressive stress versus displacement of the Ni-Ti_3AlC_2 and the Ni-Cr_2AlC composites, respectively. The addition of MAX phases gradually increased the brittle nature of the composites. Ni (Composition-A) had a yield strength of ~576 MPa, the yield strength increased to ~607 MPa in Ni-5%Cr_2AlC then decreased gradually to ~500 MPa in Ni-20%Cr_2AlC. Similarly, Ni-5%Ti_3AlC_2 had a yield strength of ~536 MPa and it decreased gradually to ~502 MPa in Ni-20%Ti_3AlC_2. At higher concentration, the yield strength of Ni-30%Ti_3AlC_2 and Ni-30%Cr_2AlC decreased sharply to ~247 MPa and ~384 MPa, respectively.

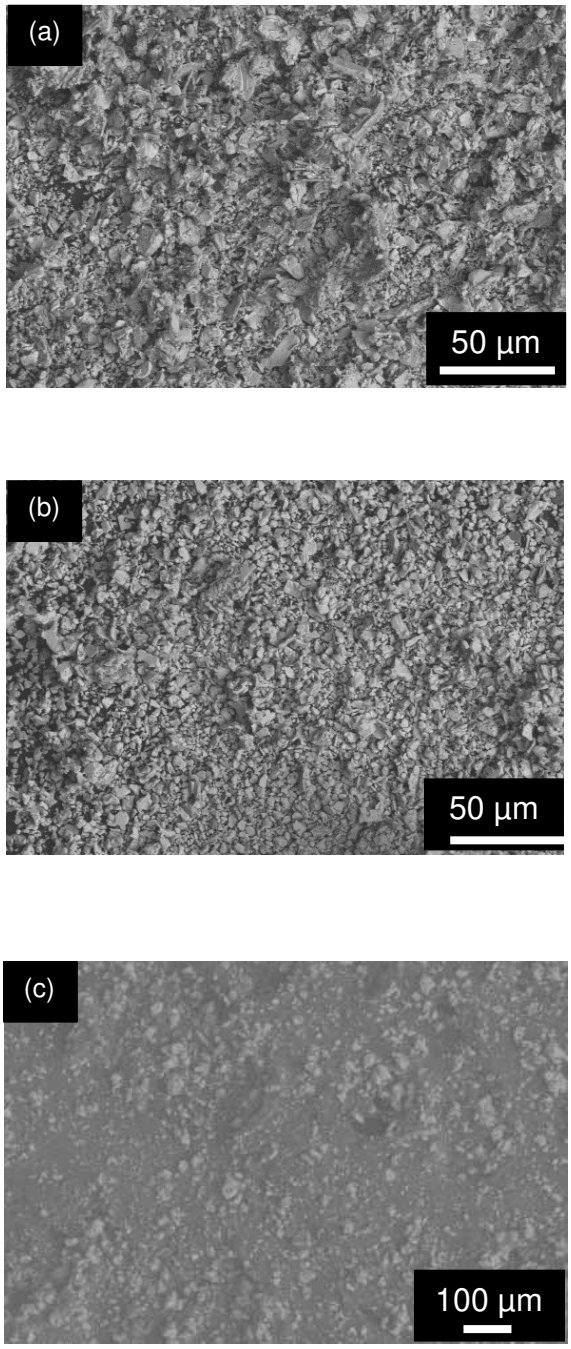

Figure 3.1: BSE SEM micrographs of, (a) Ti_3SiC_2, (b) Ti_3AlC_2, and (c) Cr_2AlC particles.

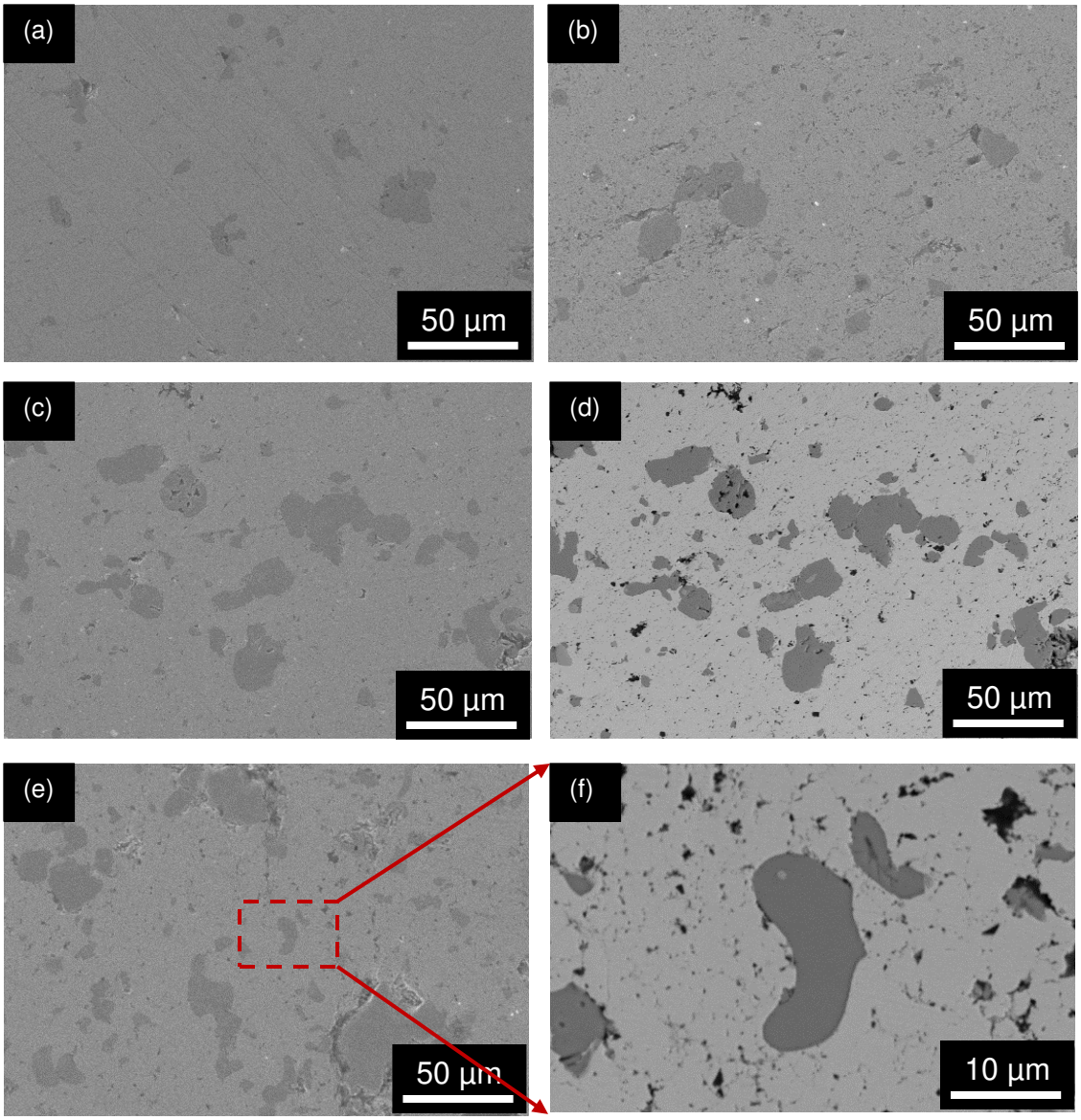

Figure 3.2: SE SEM image of, (a) Ni-5%Cr_2AlC, (b) Ni-10%Cr_2AlC, (c) Ni-20%Cr_2AlC, (d) BSE of the same region, (e) Ni-30%Cr_2AlC, and (f) BSE image of the highlighted region in (e).

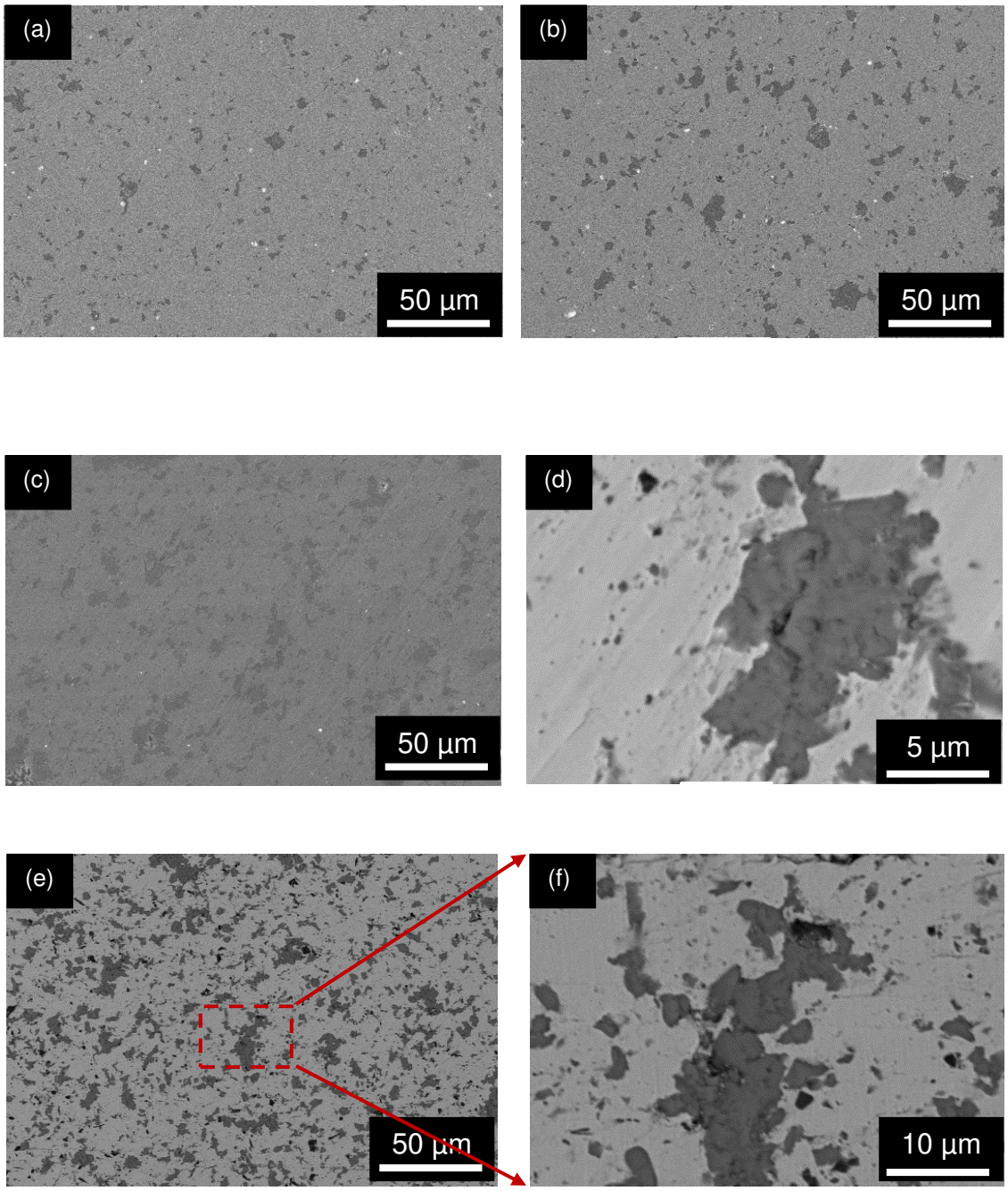

Figure 3.3: SE SEM image of, (a) Ni-5%Ti_3AlC_2, (b) Ni-10% Ti_3AlC_2, (c) Ni-20% Ti_3AlC_2, (d) BSE of the same region, (e) BSE image of Ni-30% Ti_3AlC_2, and (f) BSE image of the highlighted region in (e).

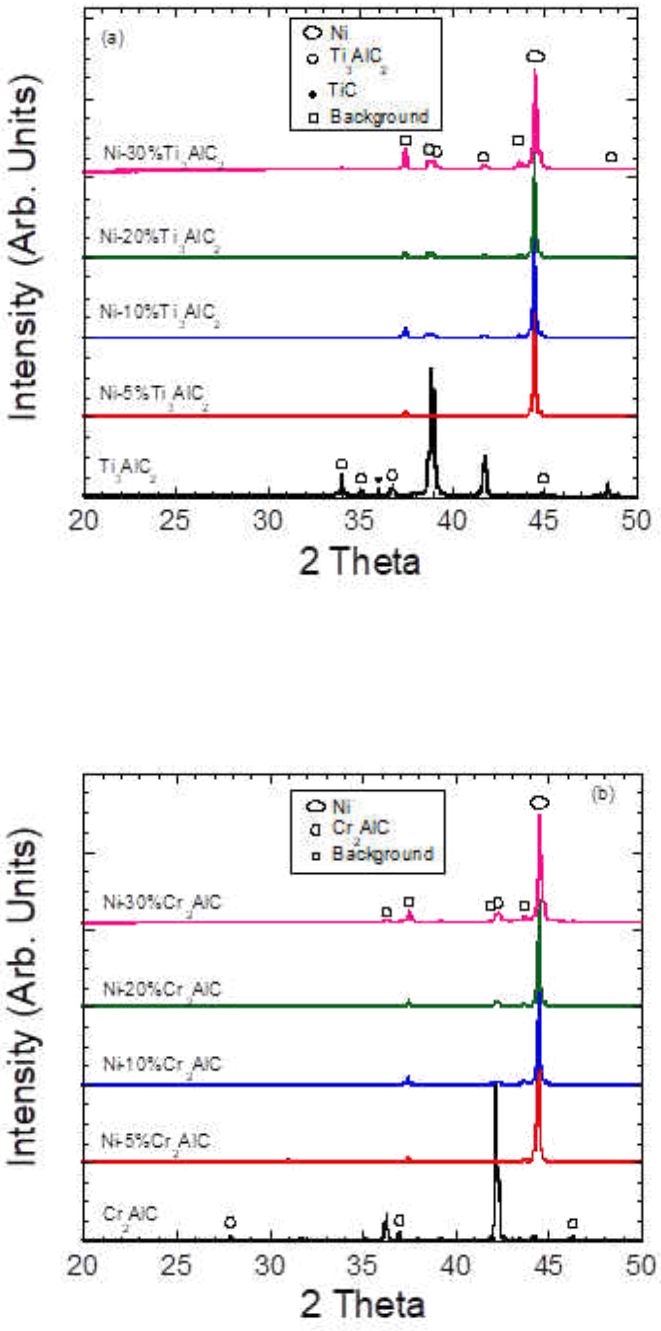

Figure 3.4: XRD plot of, (a) Ni-Ti_3AlC_2, and (b) Ni-Cr_2AlC composites.

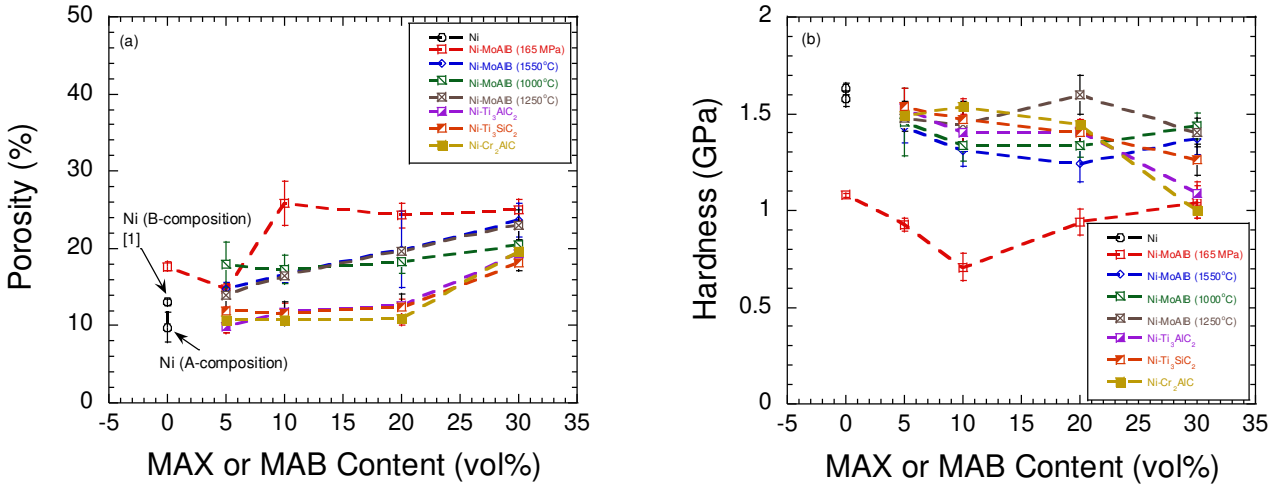

Figure 3.5: Plot of, (a) porosity, (b) hardness in Ni-matrix composites [1].

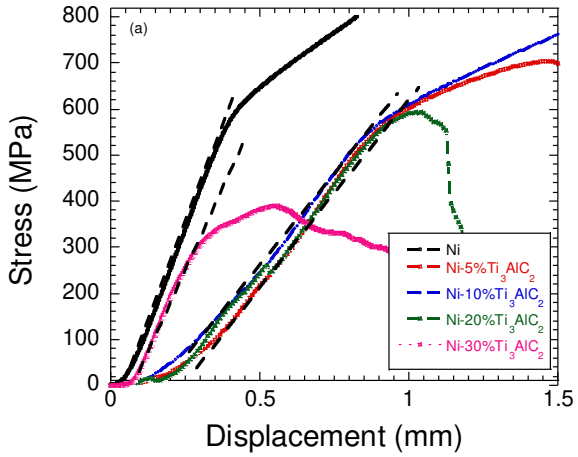

Figure 3.6: Plot of, compressive stress versus displacement in, (a) Ni-Ti_3AlC_2, (b) Ni- Cr_2AlC composites, and (c) yield strength versus MAX or MAB content (Ni-MoAlB data is from Ref. 1, and Ni-Ti_3SiC_2 data is from Chapter 2 of this thesis).

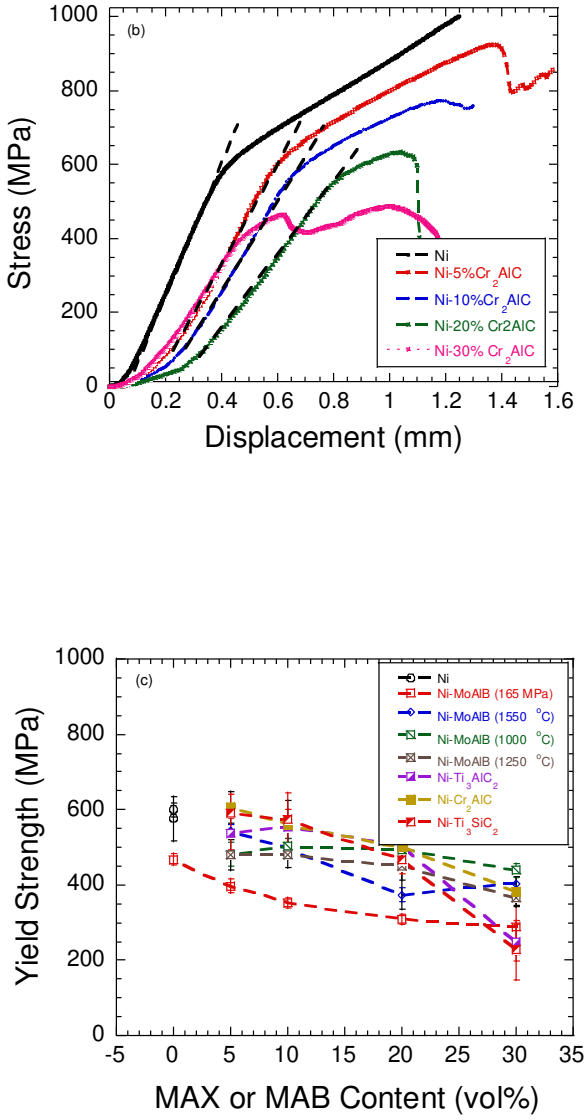

Figure 3.6: Plot of, compressive stress versus displacement in, (a) Ni-Ti_3AlC_2, (b) Ni- Cr_2AlC composites, and (c) yield strength versus MAX or MAB content (Ni-MoAlB data is from Ref. 1, and Ni-Ti_3SiC_2 data is from Chapter 2 of this thesis).

3.2.3 SUMMARY OF TRIBOLOGICAL BEHAVIOR OF DIFFERENT MRMS

Figure 3.8a shows the μ_{mean} of the Ni matrix composites. The μ_{mean} of the Ni-Ti_3AlC_2 compositions showed an abrupt increase in the μ_{mean} from ~0.55 in Pure Ni (Composition B) to ~0.77 inr Ni-5% Ti_3AlC_2, which increased to ~0.91 for Ni-10% Ti_3AlC_2. Thereafter, the μ_{mean} decreased to~0.78 in Ni-30% Ti_3AlC_2. Comparatively, in Ni-Cr_2AlC composites, the samples had similar values of μ_{mean} of ~0.55 until Ni-10%Cr_2AlC, thereafter it increased to ~0.59 and ~0.73 in Ni-20%Cr_2AlC and Ni-30%Cr_2AlC, respectively. Comparatively, Ni-Ti_3SiC_2 and Ni-MoAlB also showed a similar trend where μ_{mean} increased with the concentration of these phases (Chapter 2 and Ref. 1). Qualitatively, if we compare all the Ni-matrix composites, Ni-Cr_2AlC composites showed lower μ_{mean} than all the tested composites.

The WR of the composites are plotted in Fig. 8b as a function of MAX or MoAlB content. Comparatively, Ni-Ti_3SiC_2 and Ni-Ti_3SiC_2 are showing similar trend where WR are in the regime of (2-4) x 10^{-3} mm^3/Nm. Comparatively, the WR of Ni-Cr_2AlC fluctuates from 3 x 10^{-3} mm^3/Nm in Ni (Composition-B) to 4 x 10^{-3} mm^3/Nm in Ni-20%Cr_2AlC, thereafter it decreased by 1 order of magnitude to ~4 x 10^{-4} mm3/Nm in Ni-30%Cr_2AlC. Comparatively, Ni-MoAlB compositions also showed similar trend where the WR decreased by 1 order of magnitude in Ni-30%MoAlB. This study clearly shows that Ni-30%Cr_2AlC and Ni-30%MoAlB compositions are resistant to adhesive wear.

3.2.4 STUDY OF TRIBOFILMS AND MECHANISM OF WEAR

Figures 3.8 and 3.9 show the tribosurfaces of Ni-30%Ti_3AlC_2 versus stainless steel and Ni-30%Cr_2AlC versus stainless steel tribocouples. If we inspect the Ni-30%Ti_3AlC_2 versus stainless steel tribocouples, then wear debris and triboxides can be observed on both the Ni-30%Ti_3AlC_2 (Figs. 3.8 a-b) and stainless steel (Figs. 3.8 c-d) tribosurfaces. Comparatively, N-30%Cr_2AlC (Fig.

3.9 a-b) and stainless steel (Fig. 3.9 c-d) surface was smooth and lubricous tribofilms was observed on both surfaces. Based on this work, we can conclude that Cr_2AlC is a more effective solid lubricant than other MAX phases or MoAlB. More studies are needed to understand the detailed mechanisms responsible for these results.

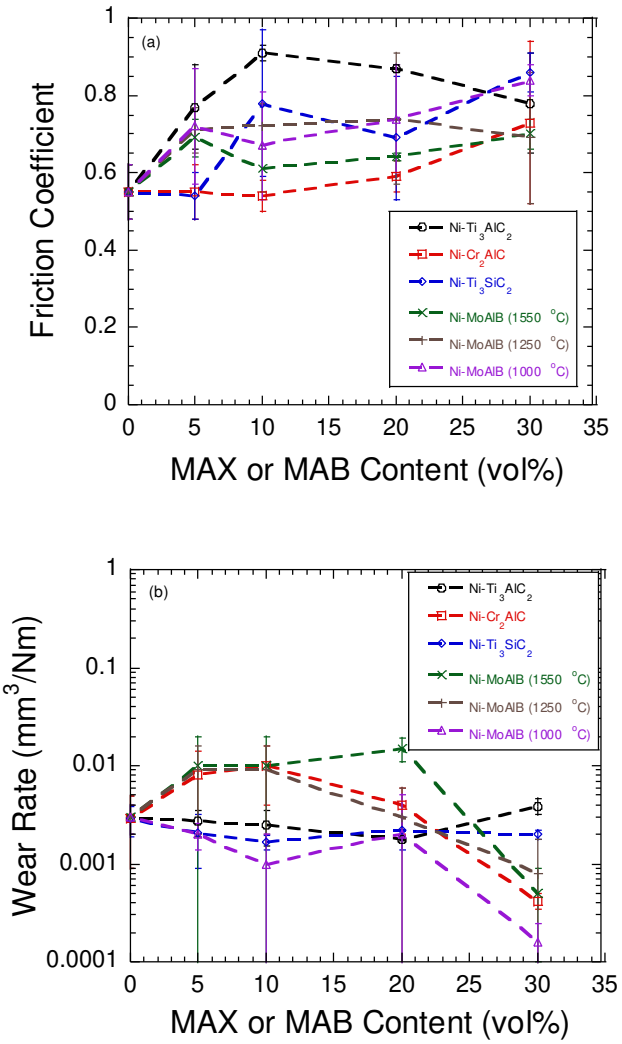

Figure 3.7: Plot of, (a) friction coefficient, and (b) WR versus MAX or MAB content in Ni-matrix composites.

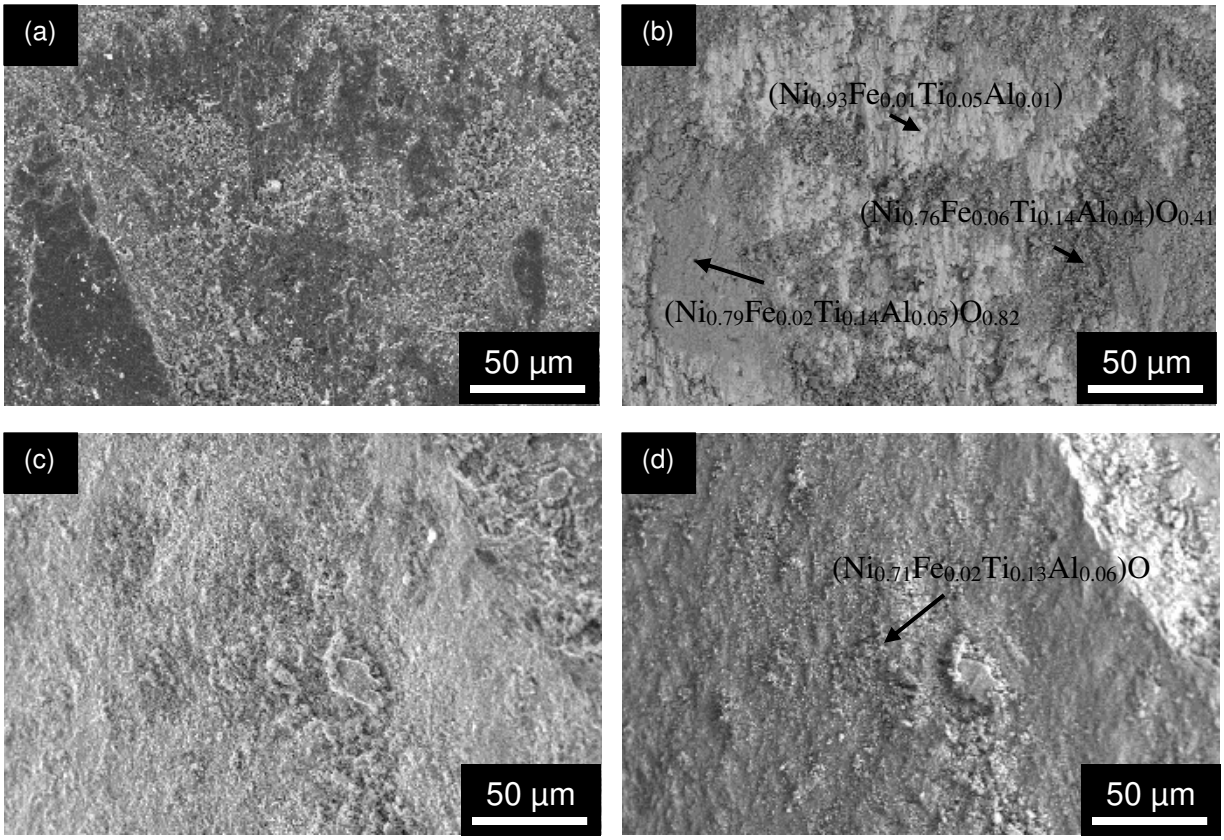

Figure 3.8: SEM of tribosurfaces of, (a) Ni-30%Ti_3AlC_2 in SE, (b) BSE of the same region, (c) steel countersurface in SE, and (d) BSE of the same region.

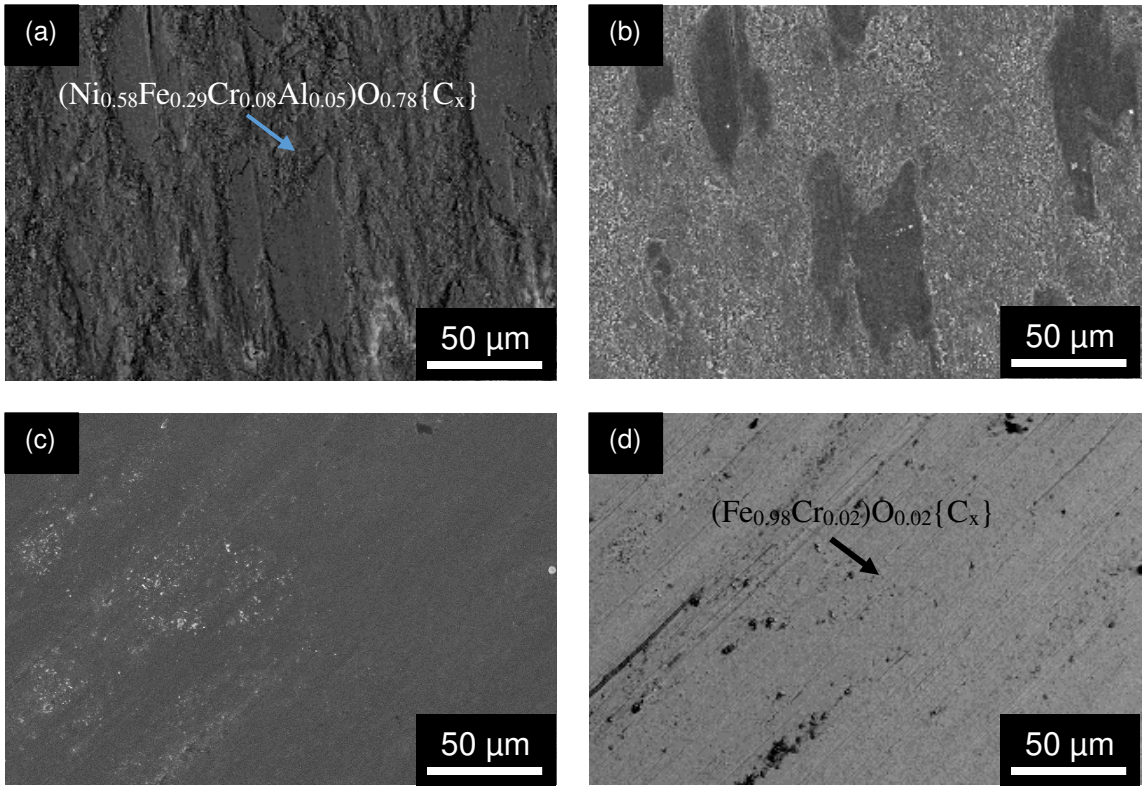

Figure 3.9: SEM of tribosurfaces of, (a) Ni-30%Cr_2AlC in SE, (b) BSE of the same region, (c) steel countersurface in SE, and (d) BSE of the same region.

CHAPTER IV

CONCLUSIONS AND FUTURE WORK

4.1 INTRODUCTION

Al-Si alloys have emerged as candidate materials for aerospace, automobile, and defense related applications, for example plain bearings, piston and cylinder liners in internal combustion engines etc. These alloys are bestowed with good thermal conductivity, mechanical behavior, and corrosion resistance [1-9]. Different metallic additives like Pb, Sn, Ti, and Cu are added to improve the mechanical and antiwear properties of AlSi alloys by engineering the microstructure [6-9]. Different researchers have also used ceramic additives like SiC, TiC and TiB_2 to enhance the mechanical and tribological behavior of these composites [10-12]. In this Chapter, we will report the tribological and mechanical behavior of AlSi-Ti_3SiC_2 composites.

4.2 EXPERIMENTAL DETAILS

Ti_3SiC_2 powder (-325 mesh, Kanthal, Hallstahammar, Sweden) and calculated amounts of Al-12wt%Si powders (Part number 88322 (-325 mesh and 99% pure), Alfa Aesar, Haverhill, MA) were initially dry mixed in a ball mill (8000 M mixer Mill, SPEX SamplePrep, Metuchen, NJ) for 5 minutes. The mixed powders were then hot-pressed under a uniaxial compressive stress of ~240 MPa (~12.7 mm die) at 500 ^oC for 10 minutes. Pure Al-12wt%Si samples were also fabricated at ~240 MPa by following procedure mentioned above. In this chapter, Al-12wt%Si composition will be referred to as AlSi. As a part of this study, ~5 vol% (Al-Si~5%312Si), ~10 vol% (Al-Si~10%312Si) and ~20 vol% (Al-Si~20%312Si) of Ti_3SiC_2 particulates were used as a reinforcement in the Al-Si alloy matrix.

The procedure for measuring porosity, mechanical behavior, hardness, and microstructure characterization by SEM is reported in Chapters II and III. In this study, the tribological study was

performed by block-on-disk tribometer (CSM Instruments SA, Peseux, Switzerland) method. The samples of AlSi-Ti_3SiC_2 compositions were cut into dimensions of ~4 mm (length) x ~4 mm (width) x ~3-4mm (height), and then polished to $R_a < 1\ \mu m$. The polished samples were tested against polished alumina disks ($R_a < 3\ \mu m$). The surface roughness of both the two surfaces were confirmed by using a surface profilometer (Surfcom 480A, Tokyo Seimitsu Co. Ltd., Japan). The experimental conditions of tribological testing were a load of 5 N, linear speed of ~50 cm/s, track radius of ~10 mm, and a sliding distance of 500 m. The mean friction coefficient was measured from each testing. For a particular composition, the mean friction coefficient from three measurements were averaged to calculate μ_{mean}. The mass of the samples and substrates were measured before and after the testing by using a weighing scale ((Model XA82/220/2X, Radwag Balances and Scales, Poland). The specific wear rate (WR) was calculated from:

$$WR = (m_i - m_f)/(\rho.N.d) \quad \text{----------(II)}$$

where, m_i is the initial mass, m_f is the final mass, ρ is density of the composite, N is the applied load, and d is the total distance traversed by the sample during the tribology testing. In this text, the total WR from both the counterparts is reported. Please refer to Chapter II about the methodology for characterizing the microstructure and tribochemistry of the worn surfaces after tribology measurements.

4.3 RESULTS AND DISCUSSION

4.3.1 MICROSTRUCTURE AND PHASE ANALYSIS

Figure 1 shows the SEM images of all the fabricated Al-Si matrix composites along with the pure Al-Si sample. All the images show that Ti_3SiC_2 particulates are uniformly dispersed in the Al-Si matrix with minimal interfacial reactions (Figs. 4.1c and 4.1f). Figure 4.2 plots porosity (Y1 axis) and hardness (Y2 axis) of the composite as a function of Ti_3SiC_2 content. The porosity

of AlSi, Al-5%Ti_3SiC_2, and Al-10%Ti_3SiC_2 had similar porosity of 4.7%, 4.4%, and 4.8%, respectively. Comparatively, the porosity of Al-20%Ti_3SiC_2Al was comparatively higher at 7.9%. The hardness of the composites also gradually increased from 924 MPa in AlSi to ~982 MPa and ~994 MPa in Al-5%Ti_3SiC_2 and Al-10%Ti_3SiC_2, respectively. Thereafter, the hardness decreased to ~909 MPa in Al-30%Ti_3SiC_2.

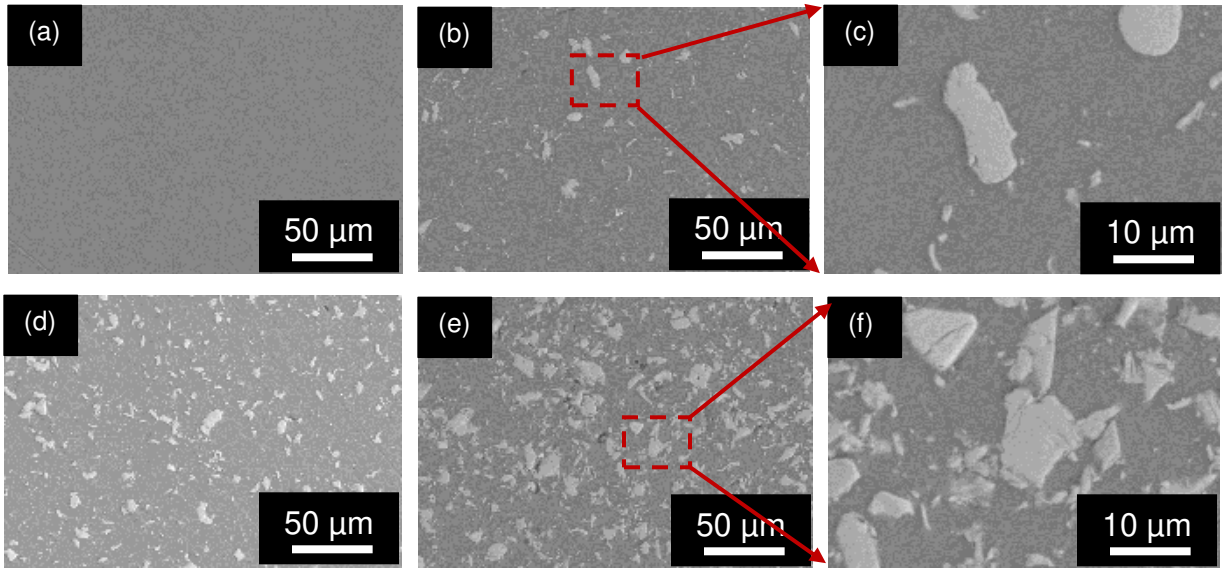

Figure 4.1: BSE SEM micrographs of, (a) AlSi, (b) AlSi-5%Ti_3SiC_2, (b) higher magnification of the marked region in (b), (c) AlSi-10%Ti_3SiC_2, (d) AlSi-20%Ti_3SiC_2, (e) higher magnification of the marked region in (e).

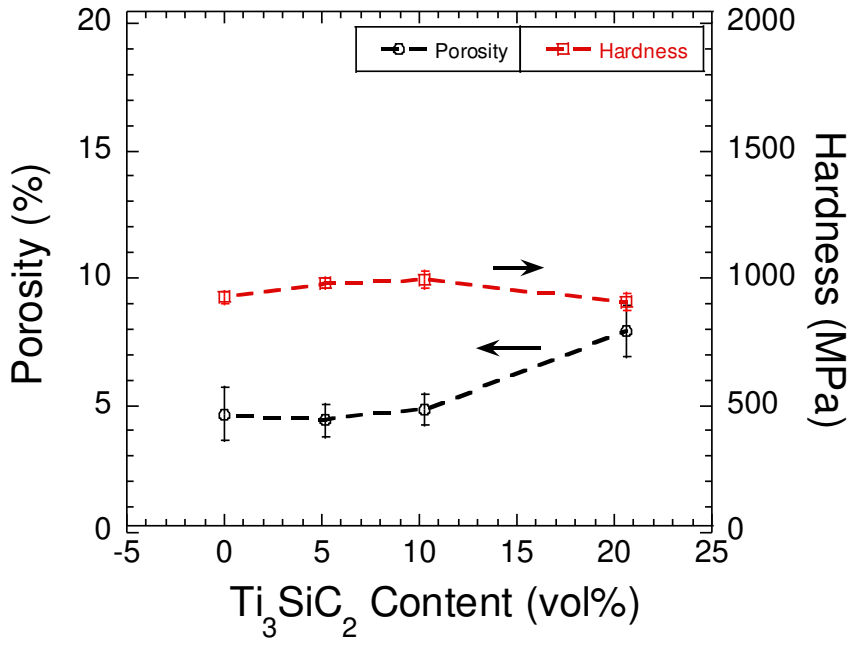

Figure 4.2, Plot of, porosity (%) (Y1 axis) and hardness (Y2 axis) as a function of Ti_3SiC_2 content.

4.3.2 COMPARISON OF MECHANICAL PERFORMANCE OF MRMS

Figure 4.3a plots the compressive stress versus displacement behavior of AlSi-Ti_3SiC_2 composites. The composites become more brittle as the content of Ti_3SiC_2 was increased in the AlSi matrix. Figure 4.3b plots the yield strength of AlSi-Ti_3SiC_2 composites as a function of Ti_3SiC_2 content. The yield strength increases from 263±26 MPa in AlSi to (283±56) MPa in Al-5%Ti_3SiC_2, thereafter it decreased to (211±106) MPa in Al-10%Ti_3SiC_2, and marginally increased to (230±94) MPa in Al-30%Ti_3SiC_2.

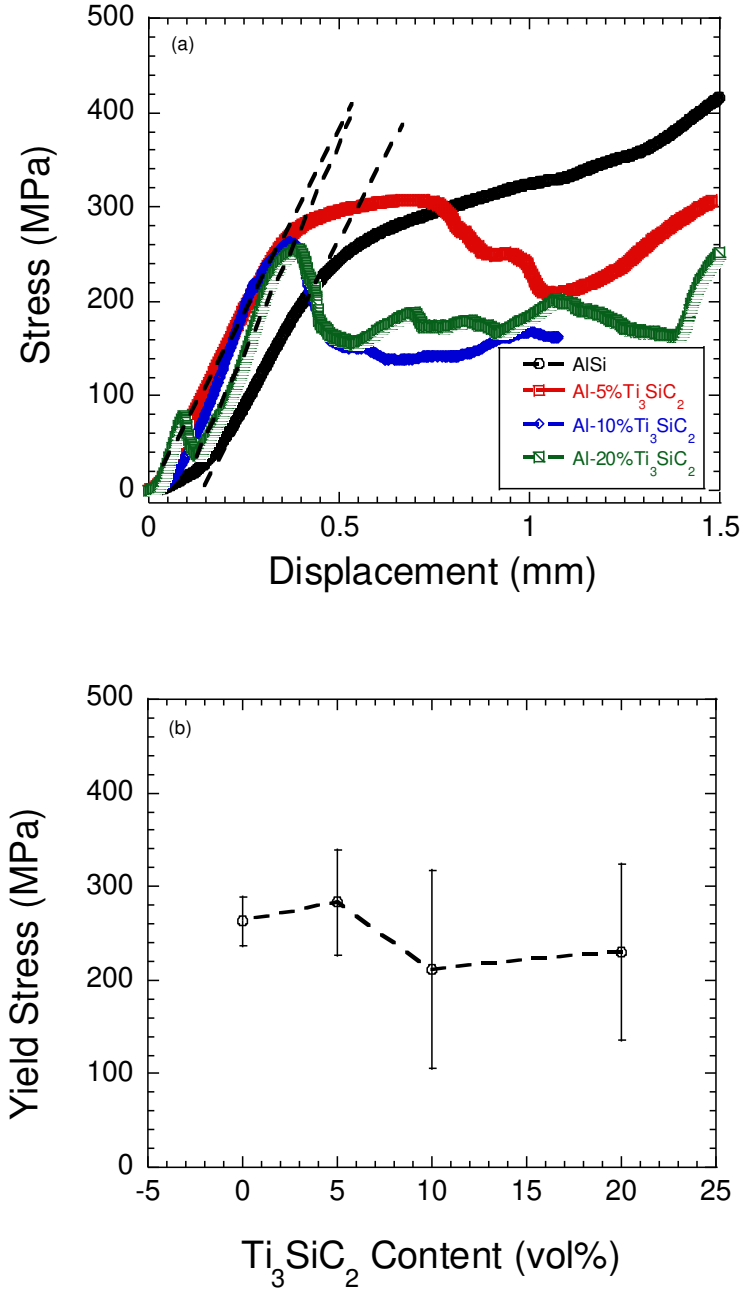

Figure 4.3: Plot of, (a) compressive stress versus displacement, and (b) ultimate compressive stress (UCS) versus Ti_3SiC_2 content in AlSi matrix.

4.3.3 SUMMARY OF TRIBOLOGICAL BEHAVIOR OF DIFFERENT MRMS

Figure 4.4a shows the plot of μ_{mean} versus the amount of Ti_3SiC_2 added in the composite. In these composites, μ_{mean} increased from ~0.56 in AlSi-5% Ti_3SiC_2 to ~0.68 in AlSi-10% Ti_3SiC_2, thereafter it decreased gradually to ~0.59 in AlSi-20% Ti_3SiC_2.

Figure 4.4b shows the plot for the wear rate of the composites. The WR of AlSi decreased marginally from ~0.0005 mm^3/Nm in AlSi to 0.0003 mm^3/Nm in Al-5%Ti_3SiC_2 thereafter it increased to ~0.0004 mm^3/Nm and 0.001 mm^3/Nm in AlSi-10%Ti_3SiC_2 and AlSi-20%Ti_3SiC_2, respectively.

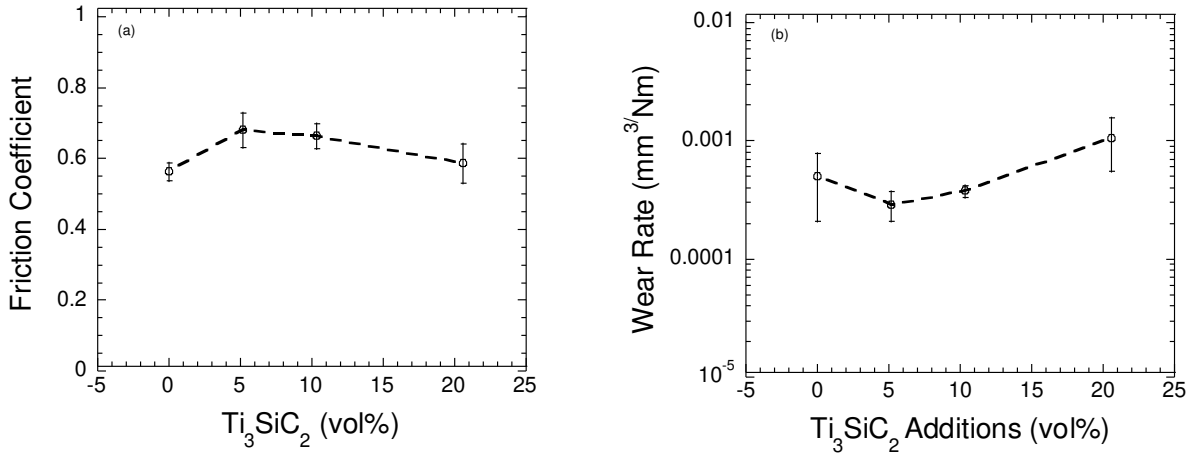

Figure 4.4: Plot of, (a) μ, and (b) WR as a function of Ti_3SiC_2 content.

4.3.4 STUDY OF TRIBOFILMS AND MECHANISM OF WEAR

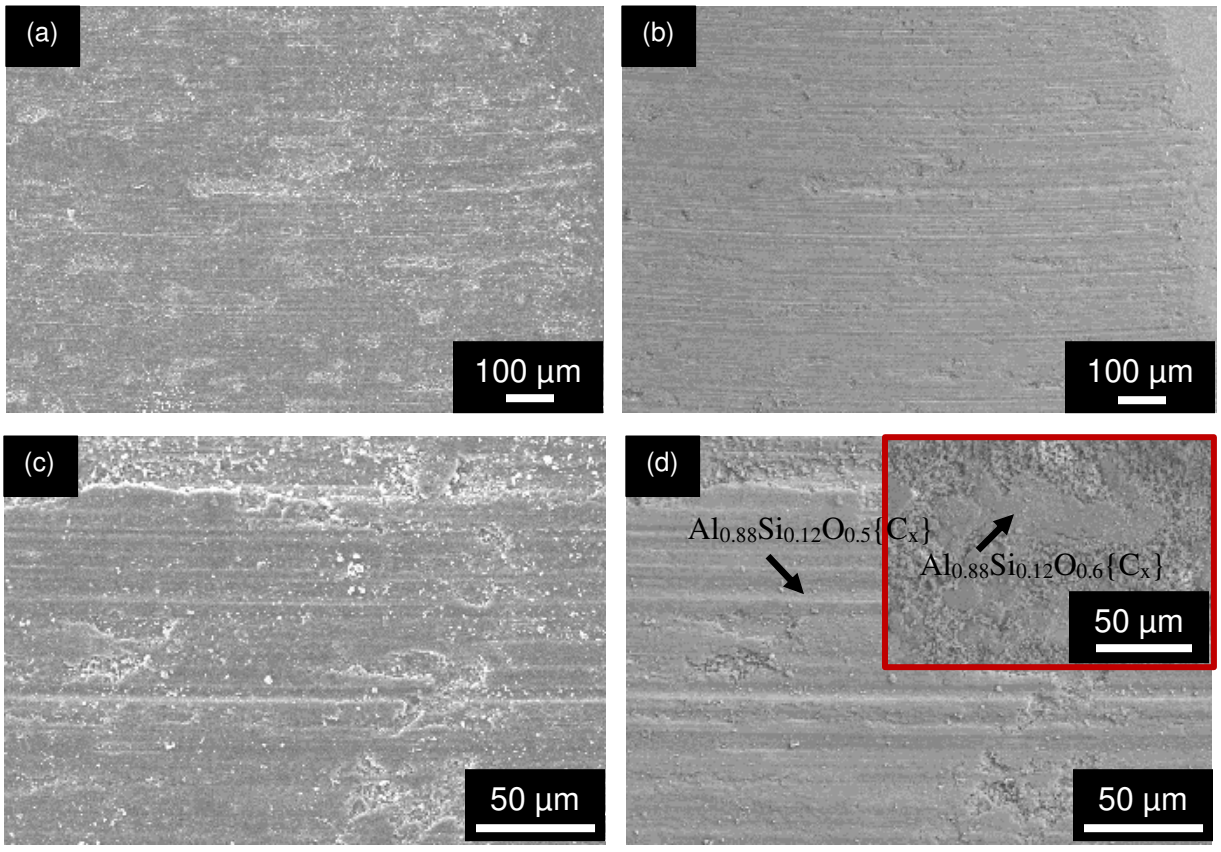

Figure 4.5: SEM micrographs of, (a) AlSi surface in SE, (b) BSE of the same region, (c) SE image of AlSi surface at high magnification, and (d) BSE of the same region (inset shows the BSE image of Al_2O_3 surface) during tribology testing.

Figures 4.5 a-d show the AlSi surface after tribological testing. The surfaces were riddled with abrasive wear tracks. Inset of Fig. 4.5d shows the alumina surface where the material transferred from AlSi surface is deposited. EDS results also show that the surface is partially oxidized. Figures 4.6 a-b and Figs. 4.6 c-d show AlSi-10%Ti_3SiC_2 and the corresponding alumina

surface after testing. It showed a similar trend like the previous case, and the material from AlSi-10%Ti_3SiC_2 surface was transferred to the alumina surface due to abrasive wear. The transferred material was also partially oxidized during the tribological testing.

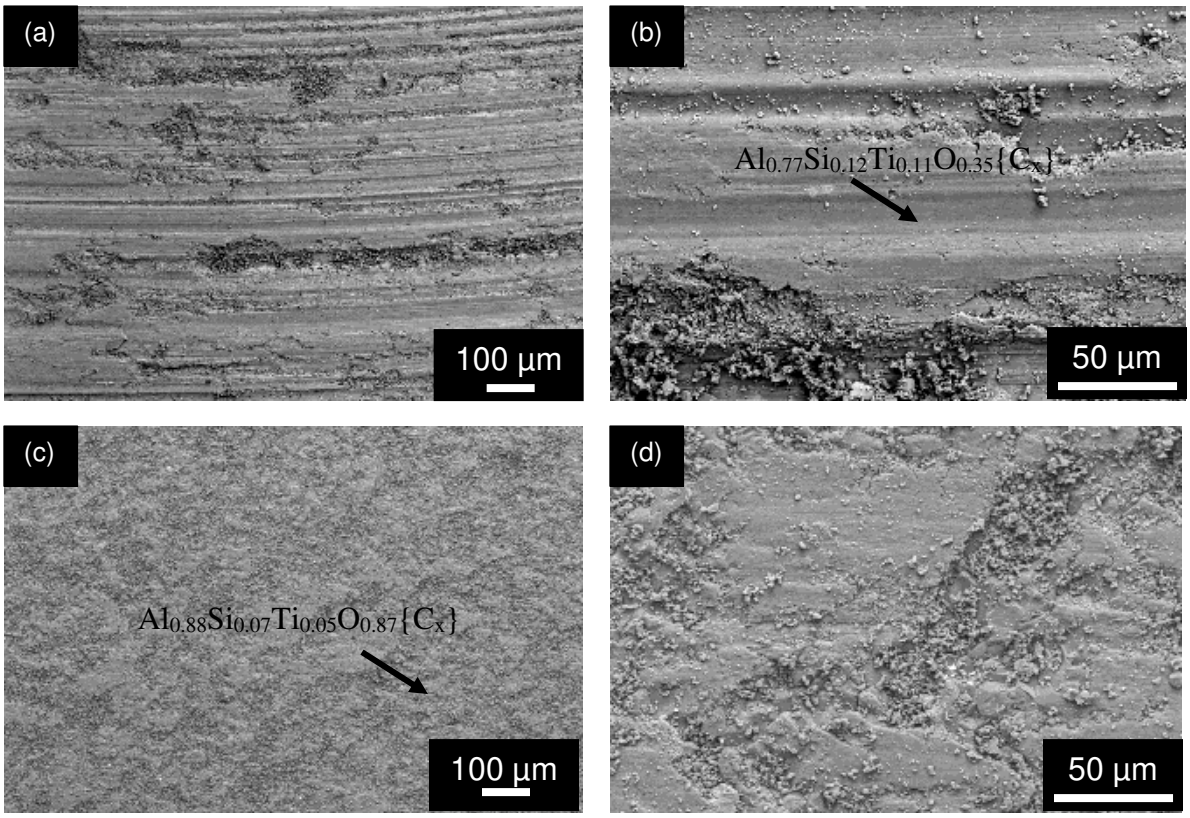

Figure 4.6: SEM micrographs of, (a) AlSi-10%Ti_3SiC_2 surface in SE, (b) BSE of the same region, (c) SE image of the Al_2O_3 surface, and (d) BSE image of the same region during tribology testing.

4.4 CONCLUSIONS

Novel AlSi- Ti_3SiC_2 composites were fabricated by hot pressing. The hot pressed samples showed higher densities than most of the previously studied MRMs. The SEM images showed that the Ti_3SiC_2 particulates were well dispersed within the AlSi matrix with minimal interfacial reactions. The addition of Ti_3SiC_2 increased the yield strength from a mean strength of ~263 MPa

for pristine AlSi to 283 MPa in AlSi-5% Ti_3SiC_2. Further addition of Ti_3SiC_2 decreased the yield strength to ~211 MPa for AlSi-10% Ti_3SiC_2, which marginally increased to ~230 MPa in AlSi-30% Ti_3SiC_2. The addition of Ti_3SiC_2 improved the tribological properties of the composite marginally. Detailed studies are needed to understand the fundamental mechanisms responsible for the observed tribological behavior.

REFERENCES

CHAPTER I

[1] R. Meng, J. Deng, R. Duan, Y. Liu, and G. Zhang, "Modifying tribological performances of AISI 316 stainless steel surfaces by laser surface texturing and various solid lubricants", *Opt. Laser Technol.*, **109**, 401-411, (2019)

[2] X. Zeng, M. Xu, and J. Li, "Examining the sustainability of China's nickel supply: 1950–2050," *Resour. Conserv. Recycl.*, **139**, 188-193 (2018)

[3] W. Hu, Z. Huang, L. Cai, C. Lei, H. Zhai, and Y. Zhou, "Exploring the interfacial state and tensile behaviors in nickel matrix composite with in-situ TiC and γ′-Ni3(Al,Ti) reinforcements", *J. Alloys Compd.*, **765**, 987-993, (2018)

[4] C. Dellacorte and J. A. Laskowski, "Tribological evaluation of PS300: A new chrome oxide-based solid lubricant coating sliding against Al_2o_3 from 25° to 650°C", *Tribol. Trans.*, **40**, 163-167, (1997)

[5] J. Zhen *et al.*, "Friction and wear behavior of nickel-alloy-based high temperature self-lubricating composites against Si_3N_4 and Inconel 718", *Tribol. Int.*, **45**, 1-9, (2014).

[6] M. W. Barsoum, *MAX phases: Properties of machinable ternary carbides and nitrides*. ISBN: 978-3-527-33011-9, (2013)

[7] M. Barsoum and T. El-Raghy, "The MAX Phases: Unique New Carbide and Nitride Materials" *Am. Sci.*, (2001)

[8] L. Hu, A. Kothalkar, M. O'Neil, I. Karaman, M. Radovic, "Current-activated, pressure-assisted infiltration: a novel, versatile route for producing interpenetrating ceramic–metal composites", Mater. Res. Lett. **2**, 124-130, (2014)

[9] A. Kothalkar, R. Benitez, L. Hu, M. Radovic, I. Karaman, "Thermo-mechanical response and damping behavior of shape memory alloy/MAX phase composites", Metall. Mater. Trans. A. **45**, 2646–2658 (2014).

[10] M.T. Agne, M. Radovic, G.W. Bentzel, M.W. Barsoum, "Stability of V_2AlC with Al in 800-1000C temperature range and ***in situ*** synthesis of V_2AlC/Al composites"**,** J. Alloys Compd., **666**, 279-286 (2016).

[11] S. Gupta, D. Filimonov, T. Palanisamy, T. El-Raghy, M. W. Barsoum, "Ta_2AlC and Cr_2AlC Ag-based Composites - New solid lubricant materials for use over a wide temperature range against Ni-based superalloys and alumina", Wear, 262, 1479-1489 (2007).

[12] T. Hammann, R. Johnson, and M.F. Riyad, "Synthesis and Characterization of Novel Al-Matrix Composites Reinforced with Ti_3SiC_2 Particulates", Journal of Materials Engineering and Performance, **24**, 1011-1017 (2014)

[13] T. Hammann, R. Johnson, M. F. Riyad, and S. Gupta, "Novel Ti_3SiC_2 reinforced Sn matrix composites", Proceedings of 39th International Conference & Expo on Advanced Ceramics & Composites (ICACC 2015).

[14] S. Gupta, M.A. Habib, R. Dunnigan, et al., "Synthesis and Characterization of Ti_3SiC_2 Particulate-Reinforced Novel Zn Matrix Composites", J. of Materi Eng and Perform, **24**, 4071-4076 (2015).

[15] S. Gupta, F. AlAnazi, S. Ghosh, R. Dunnigan, "Synthesis and Tribological Behavior of Novel Ag- and Bi- Based Composites Reinforced with Ti_3SiC_2", Wear, **376**, 1074-1083 (2017).

[16] Fuka, M. (2018) "Synthesis and Characterization of Novel Ternary Borides (MoAlB) and Their Composites" (Master's thesis). Available from ProQuest Dissertations and Theses database. (ProQuest Number: 10814246).

[17] S. Gupta, T. Hammann, R. Johnson, M.F. Riyad, "Tribological Behavior of Novel Ti_3SiC_2 (Natural Nanolaminates)-Reinforced Epoxy Composites during Dry Sliding", Tribology Transactions, **58**, 560–566 (2015).

[18] S. Gupta, S. Ghosh, and R. Dunnigan, "Synthesis and Tribological Behavior of Novel Wear Resistant PEEK-Ti_3SiC_2 composites", Journal of Engineering Tribology, **231**, 422-428 (2017).

[19] S. Ghosh, R. Dunnigan, M.A. Habib, and S. Gupta, "Novel MAX-Polymer Multifunctional Composites", Proceedings of 40th International Conference & Expo on Advanced Ceramics & Composites (ICACC 2016)

CHAPTER II

[1] "Production of nickel matrix composites reinforced with carbide particles by granulation of fine powders and mechanical pressing", M. Roseane, P. Fernandes, A. E. Martinelli, A. N. Klein, G. Hammes, Cristiano Binder, Rubens M. Nascimento, Powder Technology **305** (2017) 673–678.

[2] "Room and high temperature wear behaviour of Ni matrix micro- and nano-SiC composite electrodeposits", M. Lekka, A. Lanzutti, A. Casagrande, C. de Leitenburg, P.L. Bonora, L. Fedrizzi, Surface & Coatings Technology, **206** 3658–3665 (2012).

[3] "Mechanical behavior of α-Al_2O_3-coated SiC particle reinforced nickel matrix composites", Z. Wu, L. Liu, B. Shen, Y. Wu, Y. Deng, C. Zhong, W. Hu, Journal of Alloys and Compounds **570** (2013) 81–85.4

[4] "Tribological Evaluation of PS300: A New Chrome Oxide-Based Solid Lubricant Coating Sliding Against Al_2O_3 from 25° to 650°C", C. Dellacorte and J. A. Laskowski (1997), Tribology Transactions, **40**, 163-167, DOI: 10.1080/10402009708983642

[5] "NASA PS400: A New High Temperature Solid Lubricant Coating for High Temperature Wear Applications" C. DellaCorte and B.J. Edmonds, NASA/TM—2009-215678.

[6] "Friction and wear behavior of nickel-alloy-based high temperature self-lubricating composites against Si_3N_4 and Inconel 718", J. Zhen, F. Li, S.Zhu, Ji. Maa, Z. Qiao, W. Liu, J. Yang, Tribology International **75** (2014) 1–9.

[7] "Effects of sliding speed and testing temperature on the tribological behavior of a nickel-alloy based solid-lubricating composite", Jinming Zhen, Shengyu Zhu, Jun Cheng, Zhuhui Qiao, Weimin Liu, Jun Yang, Wear **368-369** (2016) 45–52.

[8] "MAX Phases: Properties of Machinable Ternary Carbides and Nitrides", M.W. Barsoum, John Wiley & Sons (2013).

[9] "Elastic and Mechanical Properties of the MAX Phases", M.W. Barsoum and M. Radovic Annu. Rev. Mater. Res. **41**, 195-227 (2011).

[10] "Synthesis and characterization of a remarkable ceramic: Ti_3SiC_2", M.W. Barsoum, T. El-Raghy, J. Am. Ceram. Soc. **79**, 1953–1956 (1996).

[11] M.W. Barsoum, "The $M_{n+1}AX_n$ phases: a new class of solids; thermodynamically stable nanolaminates", Prog. Solid State Chem. **28**, 201–281 (2000).

[12] "Synthesis and Characterization of Novel Al-Matrix Composites Reinforced with Ti_3SiC_2 Particulates", S. Gupta, T. Hammann, R. Johnson, and M.F. Riyad, Journal of Materials Engineering and Performance, **24**, 1011-1017 (2014).

[13] "Effect of Ti_3SiC_2 Particulates on The Mechanical and Tribological Behavior of Sn-Matrix Composites", T. Hammann, R. Johnson, M. F. Riyad, and S. Gupta, Proceedings of 39th Int'l Conf & Expo on Advanced Ceramics & Composites (ICACC 2015).

[14] "Synthesis and Characterization of Ti_3SiC_2 Particulate-Reinforced Novel Zn-Matrix Composites", S. Gupta, Habib, M.A., Dunnigan, R. et al. J. of Materi Eng and Perform, **24**, 4071-4076, (2015)

[15] "Synthesis and Tribological Behavior of Novel Ag- and Bi-based Composites Reinforced with Ti_3SiC_2" , F. AlAnazi, S. Ghosh, R. Dunnigan, and S. Gupta, Wear **376–377**, Part B, 1074-1083 (2017).

[16] "Processing and microstructure of Ti_3SiC_2 /M (M = Ni or Co) composites", H. Lia, L.M. Peng, M. Gong , L.H. He, J.H. Zhao, Y.F. Zhang, Materials Letters **59** (2005) 2647 – 2649.

[17] "On the tribology of the MAX phases and their composites during dry sliding: A review", S. Gupta and M.W. Barsoum, Wear **271**, 1878– 1894 (2011).

CHAPTER III

[1] Fuka, M. (2018) "Synthesis and Characterization of Novel Ternary Borides (MoAlB) and Their Composites" (Master's thesis). Available from ProQuest Dissertations and Theses database. (ProQuest Number: 10814246).

CHAPTER IV

CONCLUSION AND FUTURE WORK

[1] "Microstructure and mechanical properties of Al-12Si produced by selective laser melting", A S Fefelov, A G Merkushev and O A Chikova, IOP Conf. Series: Earth and Environmental Science **87**, (2017).

[2] "Microstructure and mechanical properties of Al–12Si produced by selective laser melting: Effect of heat treatment", K.G. Prashanth, S. Scudino , H.J. Klauss, K.B. Surreddi, L. Löber, Z. Wang, A.K. Chaubey, U. Kühn, J. Eckert, Materials Science & Engineering A **590**, 153–160 (2014).

[3] "Study on wear properties of aluminium–silicon piston alloy" M.M. Haque, A. Sharif, Journal of Materials Processing Technology **118**, 69–73 (2001).

[4] "Studies on the dry sliding wear behaviour of hypoeutectic and eutectic Al–Si alloys", S.A. Kori, T.M. Chandrashekharaiah, Wear **263**, 745–755 (2007).

[5] "Evolution of microstructure and its effect on wear and mechanical properties of spray cast Al–12Si alloy", K. Raju, A.P. Harsha, S.N. Ojha, Materials Science and Engineering A **528**, 7723– 7728 (2011).

[6] "Spray forming of Al–Si–Pb alloys and their wear characteristics", G.B. Rudrakshi, V.C. Srivastava, J.P. Pathak, S.N. Ojha, Materials Science and Engineering **A 383**, 30–38 (2004).

[7] "Influence of tin content on tribological characteristics of spray formed Al–Si alloys", M. Anil, V.C. Srivastava, M.K. Ghosh, S.N. Ojha, Wear **268**, 1250–1256 (2010).

[8] "Influence of Ti addition on wear properties of Al–Si eutectic alloys", N. Saheb, T. Laoui, A.R. Daud, M. Harun, S. Radiman, R. Yahaya, **249**, Wear 656–662 (2001).

[9] "Effect of copper on the tribological properties of Al-Si base alloys", J Mater Sci Lett (1995) 14: 1661. https://doi.org/10.1007/BF00422668.

[10] "Comparative investigation of microstructure, mechanical properties and strengthening mechanisms of Al-12Si/TiB_2 fabricated by selective laser melting and hot pressing", L.X. Xi , H. Zhang , P. Wang , H.C. Li, K.G. Prashanth , K.J. Lina , I. Kaban , D.D. Gu, Ceramics International **44**, 17635–17642 (2018).

[11] "Selective laser melting of in-situ Al_4SiC_4 + SiC hybrid reinforced Al matrix composites: Influence of starting SiC particle size", Fei Chang, Dongdong Gu, Donghua Dai, Pengpeng Yuan, Surface & Coatings Technology **272,** 15–24 (2015).

[12] "Selective laser melting additive manufacturing of TiC/AlSi10Mg bulk-form nanocomposites with tailored microstructures and properties", Dongdong Gu, Hongqiao Wang, Fei Chang, Donghua Dai, Pengpeng Yuan, Yves-Christian Hagedorn , Wilhelm Meiners, Physics Procedia **56,** 108–116 (2014).